Taylor & Francis
Taylor & Francis Group

The reactivity of ground-state carbon atoms with unsaturated hydrocarbons in combustion flames and in the interstellar medium

RALF I. KAISER† and ALEXANDER M. MEBEL‡

†Department of Chemistry, University of York, York YO10 5DD, UK
‡Institute of Atomic and Molecular Sciences, Academia Sinica, Taipei, Taiwan

This article reviews recent crossed-beams and *ab-initio* studies of reactions of ground-state carbon atoms $C(^3P_j)$ with unsaturated hydrocarbons and their radicals. All reactions have no entrance barrier and are initiated via an addition of the carbon atom to the π system. With the exception of the carbon atom reaction with acetylene, which also shows a significant fraction of molecular hydrogen loss, these bimolecular collisions are dominated by an atomic carbon versus hydrogen atom exchange mechanism. In some systems, homolytic cleavages of carbon–carbon bonds present additional decomposition routes of typically a few per cent at the most. The impact-parameter-dependent chemical dynamics are interpreted in terms of statistical and non-statistical decomposition of reaction intermediates involved. The polyatomic reaction products are highly hydrogen-deficient resonance-stabilized free radicals. The latter are strongly suggested as suitable precursors to form the first (substituted) aromatic ring molecule, polycyclic aromatic hydrocarbon-like species and carbonaceous nanoparticles in combustion processes, chemical vapour deposition and the outflows of carbon stars.

† Email: rik1@york.ac.uk
‡ Email: mebel@po.iams.sinica.edu.tw

1.   Introduction

The reaction dynamics involved in the formation of polycyclic aromatic hydrocarbons (PAHs) and carbonaceous nanostructures are of major relevance in understanding combustion processes [1–10], atmospheric chemistry [11, 12], chemical vapour deposition [13–20] and the chemical evolution of various extraterrestrial environments [21–25]. Carbonaceous nanoparticles are commonly referred to as soot and are often associated with incomplete combustion processes [26]. Soot is primarily composed of nanometre-sized stacks of planar layers of carbon atoms. These layers can be characterized as fused benzene rings and are probably formed via agglomeration of PAHs and possibly fullerenes [27, 28]. Once liberated into the ambient environment, soot particles in a respirable size of 10–100 nm can be transferred into the lungs by breathing and are strongly implicated in the degradation of human health [11]. This is in particular due to their high carcinogenic risk potential. PAHs and carbonaceous nanoparticles are also serious water pollutants and bioaccumulate in the fatty tissue of living organisms. Together with leafy vegetables, where PAHs and soot deposit easily, they have been linked to food poisoning, liver lesions and tumour growth. Even smaller soot particles (less than 10 nm) can be transported to high altitudes and influence the atmospheric chemistry [12]. These particles act as condensation nuclei for water ice, are thought to accelerate the catalytic degradation of ozone and lead ultimately to an increased rate of skin cancer on Earth and possibly to a reduced harvest of crops.

Polycyclic aromatic hydrocarbons [29–46] together with their cations [47–71], as well as hydrogenated [72] and dehydrogenated PAHs [73–77] are also linked to the chemical evolution of extraterrestrial environments. Currently, PAH-like species are presumed to tie up about 18% of the cosmic carbon [78, 79] and are considered as

the carrier of diffuse, interstellar absorption bands covering the visible spectrum from 440 nm to the near infrared [80]. Moreover, they might represent the emitter of unidentified infrared bands observed at 3030, 2915, 2832, 1612, 1300, 1150 and 885 cm^{-1} [81] which dominate the spectra of a T Tauri stars [82], regions of ionized hydrogen (HII regions) [83] and stars in their early (young stellar objects [84, 85]) and final stages of evolution (planetary nebulae [86–88] and circumstellar envelopes of carbon stars [89–94]). These molecules are further considered as precursors, leading to carbonaceous grain material with various degrees of hydrogenation [95–103] and possibly to fullerenes [104–109]. Here, PAH-like material is thought to be formed in outflow of dying carbon-rich stars and to shield molecules from the destructive interstellar radiation field; carbonaceous nanoparticles are suggested also to serve as catalysts to synthesize molecular hydrogen. The crucial role of nanodiamonds in interstellar space [110–112] and in chemical vapour deposition on the industrial scale [13–20] should be noted as well.

However, despite the key role of PAHs and carbonaceous nanoparticles in industrial processes and in numerous (extra)terrestrial settings, no conclusive evidence has been given so far on their formation processes. The synthesis of small carbon-bearing radicals is thought to be linked to the formation of PAHs and ultimately soot production in combustion flames [113, 114]. These pathways might be similar to those processes forming PAH structures in extraterrestrial environments. Synthetic routes are proposed to involve a successive build-up of hydrogen-deficient carbon bearing radicals via sequential addition steps of ground-state atomic carbon C(^{3}P$_j$), carbon molecules (C$_2$ and C$_3$), and small hydrocarbon radicals (C$_2$H, C$_2$H$_3$, C$_3$H, C$_3$H$_2$, C$_3$H$_3$, C$_3$H$_5$ and C$_6$H$_5$) and reactions via acetylene (C$_2$H$_2$), benzene (C$_6$H$_6$), PAH-like structures and fullerenes [115–117]. Chemical reaction networks modelling PAH formation suggest further a stepwise extension of monocyclic rings via benzene (C$_6$H$_6$), phenyl (C$_6$H$_5$) and/or cyclopentadienyl radicals (C$_5$H$_5$) to polycyclic systems [118–122]. Even the most fundamental mechanisms on the formation of these very first cyclic building blocks via hydrogen-deficient C$_2$ to C$_5$ radicals such as propargyl (C$_3$H$_3$) [123–128], allyl (C$_3$H$_5$) [129] or various C$_4$H$_3$ and C$_4$H$_5$ isomers [130–138] have not been well understood nor included systematically into reaction networks which model the formation of PAHs and carbonaceous nanostructures. This is because solid laboratory data on rate constants, reaction products and intermediates involved are sparse.

Bimolecular reactions of ground-state carbon atoms C(^{3}P$_j$) with unsaturated hydrocarbons and their radicals are of particular importance. Atomic carbon is the fourth most abundant element in the Universe and is ubiquitous in the interstellar medium. Carbon atoms have been detected via their 609 μm ^{3}P$_1$–^{3}P$_0$ transition in significant amounts in, for instance, circumstellar envelopes of the carbon stars IRC + 10216 and α Orionis [139–142], towards the proto planetary nebulae CRL 618 and CRL 2688 [143], in the diffuse cloud ζOph [144], and towards the dense cloud OMC-1 [145]. In terrestrial environments such as oxidative hydrocarbon flames, the transient carbon atoms are also assumed to contribute significantly to combustion processes [146]. The reactions of carbon atoms with unsaturated hydrocarbons are strongly expected to open prompt routes to form hydrocarbon radicals with multiple carbon–carbon bonds and, in particular, resonance-stabilized free radicals (RSFRs) such as the propargyl (C$_3$H$_3$) or the *n*-C$_4$H$_3$ radicals. Both open-shell species are believed to play a crucial role in the formation of aromatic compounds, PAHs and soot in the combustion of aromatic fuels [147–171]. In

RSFRs, the unpaired electron is delocalized and spread out over two or more sites in the molecule. This results in a number of resonant electronic structures of comparable importance. Owing to the delocalization, resonance-stabilized free hydrocarbon radicals are more stable than ordinary radicals, have lower enthalpies of formation and normally form weaker bonds with stable molecules (including molecular oxygen) [166, 167, 171–174]. Such weakly bound addition complexes are not easily stabilized by collisions at high temperature. Consequently RSFRs are relatively unreactive and can reach a high concentration in flames. These high concentrations and the relatively fast rates of the RSFR + RSFR reactions make them an important mechanism to form complex hydrocarbons in flames.

For instance, the self-reaction of the simplest and most important RSFR, propargyl, is generally believed to be the most significant cyclization step in flames of aliphatic fuels and in outflow of circumstellar envelopes [175–181]. Current models of combustion flames and carbon-rich outflows postulate that soot formation and synthesis of PAH are initiated by recombination of two propargyl radicals to C_6H_6 isomers followed by unimolecular rearrangements. However, the synthetic route to form the propargyl is far from being completely understood. Various reactions were suggested, such as the reactions of $CH(X\,^2\Pi_\Omega)$ and $CH_2(a\,^1A_1)$ with acetylene, and the thermal decomposition of allene or methylacetylene via carbon–hydrogen bond rupture [182–185]. However, the reaction of the ground-state carbon atoms with ethylene is a viable alternative [186]. Many other RSFRs postulated to be important in the cyclization and PAH growth processes are substituted propargyl radicals such as methylpropargyl [166, 167, 170], which can also be produced in the reaction of carbon atoms with unsaturated hydrocarbons. Another RSFR is C_4H_3 which can be synthesized in the reactions of carbon atoms with allene and methylacetylene. In oxygen-deficit combustion flames the iso and normal C_4H_3 isomers are expected to play a crucial role in the formation of the phenyl radical (C_6H_5) via the three-body reaction with acetylene (C_2H_2) [155, 187, 188]. Starting from the phenyl radical, the growth of PAH molecules is thought to involve different variations of the hydrogen abstraction–acetylene addition (HACA) sequences [150, 151, 171, 189–192]. Acetylene, vinylacetylene and polyacetylenes were found to be the major species in such a stepwise synthesis, which starts from acetylene polymerization, leading to chain lengthening and formation of unsaturated radical species. These active radicals are then suggested to form aromatic rings by ring closure or cyclization reactions. An alternative mechanism is the formation of branched hydrocarbon radicals with side chains, which undergo subsequent ring closure, giving an aromatic ring with a two-carbon side chain (e.g. phenylacetylene). In further synthesis, reactions among the growing aromatic species, such as radical recombination and addition, are postulated to give a wide variety of PAHs. Besides acetylene and polyacetylenes, other C_2 hydrocarbons (ethynyl and vinyl) and also C_3 (propargyl and propargylene), C_4 (1,3-butadiene and 1,3-butadienyl), C_5 (cyclopentdienyl) and C_6 (fulvene) species were found to give considerable contribution to the formation of the first aromatic ring and consequently condensed aromatic systems [171]. Meanwhile, these species can be also produced in the reactions of atomic carbon with unsaturated hydrocarbons. For example, diacetylene can be formed in the reaction of carbon atoms with the propargyl radical.

Naphthalene and larger PAH molecules might be produced not only by the HACA mechanism but also as a result of recombination and subsequent rearrangements of cyclopentadienyl (C_5H_5) radicals [161–163, 193]. The recombination of two

C_5H_5 radicals is thought to be followed by a hydrogen atom loss leading to the resonance-stabilized C_5H_5–C_5H_4 radical, which then rearranges to naphthalene. A similar pathway, including the reaction of cyclopentadienyl with indenyl was suggested for the phenanthrene formation [161, 162, 194]. A simpler reaction of cyclopentadienyl with methyl radicals can produce fulvene [163, 195], a probable precursor of benzene [167, 196, 197]. Despite the great importance of the cyclo-pentadienyl radical, surprisingly little is known about its formation mechanism. In combustion flames, a possible reaction path involves oxidation of the phenyl radical (which itself is formed via activation of benzene by abstraction of a hydrogen atom) by molecular oxygen [198]. Alternative mechanisms, where C_5H_5 is produced from smaller unsaturated hydrocarbons, include the $C_3H_3 + C_2H_2$ and $C_3H_4 + C_2H_2$ reactions as well as the reaction of the ground-state atomic carbon with various C_4H_6 isomers. Therefore, new models of various chemical processes in flames and in extraterrestrial environments should inevitably include the $C(^3P_j)$ reactions with unsaturated hydrocarbons. These reactions are expected to affect significantly the concentration of unsaturated and resonance-stabilized radical hydrocarbon species and thus to influence the formation and growth of PAHs and carbonaceous nanoparticles in combustion processes and various extraterrestrial environments.

However, to assess once and for all the role of bimolecular reactions of small hydrocarbons and their radicals with carbon atoms to form PAHs and their precursors, three sets of data are crucial. These are

  (i) temperature-dependent rate constants,
 (ii) the identification of the reaction products and
(iii) an assignment of reaction intermediates.

Kinetic studies on the reactivity of ground state carbon atoms pointed out that all reactions proceeded with second-order kinetics and are very rapid ($k = 2.9 \times 10^{-10}$–$1.5 \times 10^{-9}\,cm^3\,s^{-1}$) [199–209]. A systematic data analysis combin-ing the absolute rate constants with classical capture theory dominated by an isotropic dispersion term suggested further that these reactions have no entrance barrier and progress close to the gas kinetics limits [210]. These investigations were extended also to temperatures as low as $7\,K$ [211–220]. The magnitudes of the rate constants of $(2.9–4.8) \times 10^{-10}\,cm^3\,s^{-1}$ recommend that, even at these low tempe-ratures, atomic carbon reacts in a barrierless manner and rapidly with unsaturated molecules; the reactions of carbon atoms follow further a general trend of slightly increasing rates as the temperature drops. This was proposed to be consistent with the formation of an initial collision complex speculated to be initiated by an addition of $C(^3P_j)$ to the unsaturated bond of the reactant with a rate determined by a capture process. Finally, the low-temperature studies propose further that all three spin–orbit states of the carbon atom $C(^3P_0)$ ($0\,cm^{-1}$), $C(^3P_1)$ ($+16.4\,cm^{-1}$), and $C(^3P_2)$ ($+43.4\,cm^{-1}$) react at comparable rates with unsaturated hydrocarbons.

Although these kinetic experiments provided unprecedented information on temperature dependent rate constants, their crucial drawback is the missing in-formation on intermediates involved, reaction products and branching ratios. Therefore, information on the chemical reaction dynamics under single-collision conditions as provided in crossed-molecular-beams experiments are crucial to provide this information. This review article presents an overview of recent crossed-beams experiments and theoretical studies on the chemical dynamics of bimolecular reactions of carbon atoms with unsaturated hydrocarbons and their

radicals. These investigations provide intimate insights into the underlying reaction mechanisms at the molecular level—a crucial piece of information to untangle the chemical processing and formation of PAHs and their precursor molecules in combustion flames and distinct extraterrestrial environments.

2. Experimental method

Since the formation of PAHs and their precursors consists of multiple elementary reactions, which are a series of bimolecular encounters between atoms, radicals and closed-shell species, only a detailed knowledge of the reaction mechanisms at the most fundamental microscopic level provides a comprehensive understanding on how these molecules are formed from the 'bottom-up' via single atoms and radicals. The crossed molecular beam technique represents the most versatile approach to elucidate these chemical dynamics of elementary gas-phase reactions [221–224]. In contrast with bulk experiments, where reactants are mixed, the main advantage of a crossed-beams machine is the capability to prepare atoms and radicals (the building blocks of each PAH and carbonaceous nanoparticle) in separate supersonic beams in well-defined quantum states before they cross at a specific collision energy under single-collision conditions. The species of each beam are made to collide only with the molecules of the other beam, and the products formed fly undisturbed towards the detector. These features provide an unprecedented approach to observe the consequences of a single molecular collision, preventing secondary collisions and wall effects. These reaction conditions occur especially in dense interstellar clouds where the low number densities of less than 10^4 atoms cm^{-3} support only binary reactions; three-body encounters are absent [225]. However, in denser combustion flames, circumstellar envelopes, planetary nebulae or planetary atmospheres, three-body collisions may occur, and any reaction intermediate could be stabilized or, since these transient species are often radicals, react, leading to more complex molecules. Therefore, these intermediates must also be identified to obtain a complete picture on the chemical processes involved in the formation of PAHs and their precursors. Hence, the experiments allow also us to discriminate whether a bimolecular reaction is indirect via reaction intermediate(s) or direct through a transition state.

A typical top view of a crossed-molecular-beams machine is displayed in figure 1 [224, 225]. This set-up consisting of two source chambers fixed at 90° crossing angle, a stainless steel scattering chamber and an ultrahigh-vacuum rotatable, triply differentially pumped quadrupole mass spectrometry detector. In the primary source, a pulsed supersonic $C(^3P_j)$ beam is produced via laser ablation of graphite employing a neodymium-doped yttrium aluminium garnet laser at a 30 Hz repetition rate at 266 nm [226] and seeding the ablated species into helium or neon nitrogen carrier gas released by a pulsed valve. This pulsed primary beam passes through a skimmer into the main chamber of the machine. A four-slot chopper wheel is located after the skimmer and selects a slice of well-defined velocity and velocity spread from the primary beam which reaches the interaction region. Here, the atomic carbon reactant collides at a right angle with the second pulsed beam of an unsaturated hydrocarbon or hydrocarbon radical. Vinyl, $C_2H_3(X\,^2A')$ and propargyl, $C_3H_3(X\,^2B_1)$, for instance, are generated by photolysing a helium–vinyl bromide or helium–propargyl bromide mixture at 193 nm after the nozzle of the second pulsed valve. Typically, supersonic beams are characterized by very low translational
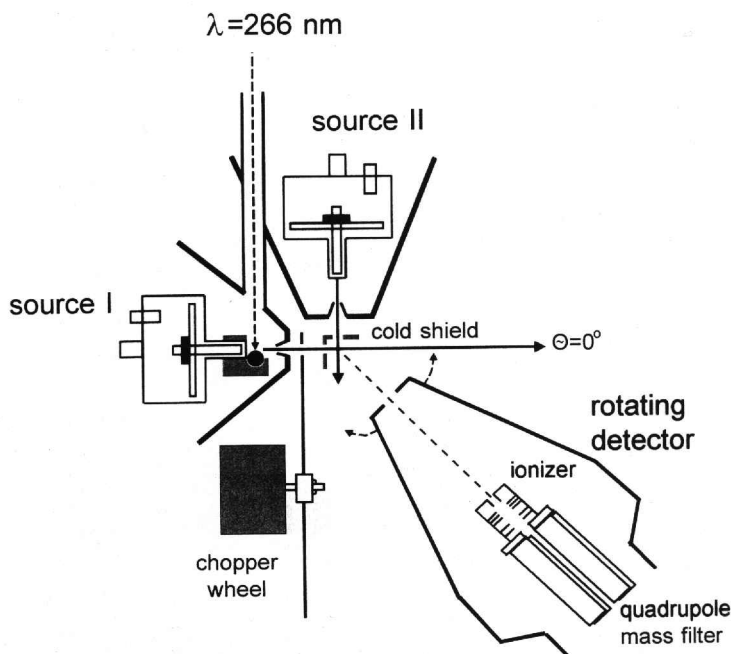
Figure 1. Schematic top view of a typical crossed-molecular-beams machine with source chambers, chopper wheel, and interaction region.

temperatures ($T < 10$ K) and rotationally and vibrationally cold reagents. Recall that the beams collide in the interaction region not at a kinetic temperature (Maxwell–Boltzman distribution), but at a collision energy as defined by the mass and velocity of each reactant. Very recently, discharge techniques have been employed to generate a continuous carbon beam [227].

The reactively scattered species are detected by a rotatable and triply differentially pumped detector at an extreme ultrahigh vacuum of less than 8×10^{-13} mbar consisting of a liquid-nitrogen-cooled electron impact ionizer followed by a quadrupole mass detector and a Daly-type detector. Any species scattered from the interaction region after a single collision event took place can be ionized in the electron impact ionizer and, in principle, it is possible to determine the gross formula of all the products of a bimolecular reaction by varying the mass-to-charge ratio m/e in the mass filter. A considerable advantage of the crossed-beams set-up with respect to common flow reactors coupled with a mass spectrometer makes it possible to measure the velocity distribution of the products. This 'time-of-flight' (TOF) operation of the quadrupole mass detector records the time-dependent ion current of a defined m/e ratio taking the crossing time of both beams in the interaction region as a well-defined time zero. Ions of the selected m/e arriving early are fast, whereas ions arriving late have low velocities; this allows one to derive the amount of the total energy available to the products and, therefore, the energetics of the reaction. The quadrupole mass detector is rotatable in the scattering plane as defined by both beams. Taking TOF spectra at one m/e at different laboratory angles and integrating these data supplies the laboratory angular distribution, that is the integrated intensity of a TOF spectrum versus the laboratory angle. In addition,

reaction products with often unknown spectroscopic properties such as polyatomic open-shell hydrocarbon radicals have to be detected. Hence, the majority of the products cannot be examined by optical detection schemes, and the mass spectro- metry detector is advantageous. Because of the mass spectrometry detector, it is often useful to probe the heavy reaction product. Note that, very recently, crossed- beam experiments of atomic carbon with unsaturated hydrocarbons probing the atomic hydrogen and deuterium products via laser-induced fluorescense have been conducted [228, 229].

For the physical interpretation of the involved reaction mechanism and an identification of the intermediates together with the reaction products it is essential to convert the laboratory data (the angular distribution and the TOF spectra) into the centre-of-mass reference frame. This procedure assumes initial angular $T(\theta)$ and translational energy $P(E_T)$ distributions in the centre-of-mass reference frame. TOF spectra and laboratory angular distributions are then calculated from these centre- of-mass functions, averaging over the apparatus and beam functions until a satisfactory fit of the laboratory data is achieved. The final output of the experiment is the generation of a product flux contour map. This plot relates the differential cross-section (the intensity of the reactively scattered products) $I(\theta, u) \propto P(u)T(\theta)$, as the intensity as a function of angle θ and product centre-of-mass velocity u to the centre-of-mass functions. Whereas important reaction intermediates are implied indirectly, the reaction products are identified, in the simplest case, from the $P(E_T)$ function.

The centre-of-mass functions help us to unravel the chemical reaction dynamics. Here, we compile only the most important features of fundamental interest for the astrochemistry and combustion community. To collect information on the energetics of the reaction, we investigate the centre-of-mass translational energy distribution. If the energetics of the product isomers are well separated, the maximum translation energy E_{max} can be used to identify the nature of the products. E_{max} presents the sum of the reaction exoergicity plus the experimental collision energy. Therefore, if we subtract the collision energy from the experimentally determined E_{max}, the exoergi- city of the reaction can be calculated. The distribution maximum of the $P(E_T)$ might give the order of magnitude of the barrier height in the exit channel. If a $P(E_T)$ peaks at zero or close to zero, the bond rupture has either no or only a small exit barrier (loose exit transition state). $P(E_T)$ values could show pronounced maxima away from zero translational energy, suggesting a significant electron density change from the fragmenting intermediate to the products (tight transition state). The $T(\theta)$ value provides information on the intermediates involved and is dictated by the disposal of the total angular momentum. Several shapes of the flux distributions are feasible. $T(\theta)$ values can depict a symmetric profile around 90°. This 'forward–backward' symmetric pattern is characteristic of a bimolecular reaction which goes through an intermediate (indirect scattering dynamics) having a lifetime larger than its rotation period. Alternatively, a symmetric distribution around 90° could be interpreted in a way that the reaction proceeds through a 'symmetric' exit transition state. In this case, the decomposing complex must have a rotation axis which interconverts. Alternatively, the angular flux distribution can be asymmetric around 90°. Often, the flux at 0° is larger than at 180°, suggesting a so-called 'osculating complex model'; the reaction is indirect, but the lifetime of the intermediate is of the order of the rotation period. Note that indirect reactions are often related to the deep potential energy well of a bound intermediate. Finally, the centre-of-mass angular distribution

might depict flux only in the forward direction, that is the flux peaks at 0° and is zero at larger angles ('stripping dynamics'), or only in the backward direction, that is the flux distribution shows a maximum at 180° and falls to zero at lower angles ('rebound dynamics'). Here, the reaction is 'direct' and either proceeds via a very short-lived, highly rovibrationally excited intermediate with a lifetime of less than 0.1 ps or goes through a transition state without involving an intermediate. Direct reactions are often associated with repulsive or weakly attractive potential energy surfaces (PESs).

3. Computational methods
3.1. *Ab-initio calculations of potential energy surfaces*

To unravel the chemical dynamics of complex polyatomic reactions comprehensively, it is always useful to combine the crossed-beams data with electronic structure calculations on the PESs. When *ab-initio* molecular orbital or density functional theory (DFT) calculations are used to study PESs of reactions of $C(^3P_j)$ with unsaturated hydrocarbons as considered in the present review, the reliability of the results is critical. On account of the great progress made in the field of computational chemistry in the recent decade, it is now possible to perform calculations of PESs for the reactions between small- and medium-sized molecules and radicals to chemical accuracy. This can be achieved by using multireference configuration interaction (MRCI) [230, 231] or coupled-cluster [232, 233] techniques with large correlation consistent basis sets [234]. An alternative to these computationally intensive and costly approaches is to use so-called theoretical model chemistries [235] combining high level *ab-initio* calculations with a few empirical corrections. The methods of calculations that we applied for the studies of the reactions of atomic carbon with unsaturated hydrocarbons belong to the family of Gaussian-2 (G2) [236–239] and Gaussian-3 (G3) [240–248] model chemistries. The G2 methodology uses a series of quadratic configuration interaction singles plus doubles with perturbative triples (QCISD(T)) and fourth-order Møller–Plesset (MP4) and second-order perturbation theory Møller–Plesset (MP2) calculations with various basis sets to approximate a QCISD(T)/6-311 + G(3df, 2p) single point energy at the MP2/6-31G(d) optimized geometrical structures with an additional empirical 'higher-level correction' (HLC) depending on the number of paired and unpaired electrons in the system. The accuracy of the G2 approach has been assessed by calculations of 148 molecules with well-established enthalpies of formation, which showed an average absolute deviation of 6.6 kJ mol^{-1} [249]. For a set of 146 well-established ionization potentials and electron affinities, G2 calculation gave an average absolute deviation of 5.8 kJ mol^{-1} [250]. In the G3 scheme, the 6-311 + G(3df, 2p) basis set is replaced by specially optimized 'G3-large' basis set and the accuracy slightly improves to 4–5 kJ mol^{-1}.

Recent developments in DFT enabled one to modify and improve further the performance of G2 [251, 252] and G3 [242, 241]. In the modified G2 methods (G2M) [253], geometries are optimized and vibrational frequencies are calculated using the hybrid density functional B3LYP/6-311G(d, p) approach, that is Becke's three-parameter non-local exchange potential [254] in conjunction with the non-local correlation potential of Lee, Yang and Parr [255] (B3LYP). For geometrical parameters, the B3LYP method normally provides the accuracy of 0.01–0.02 Å for bond lengths and 1–2° for bond angles and dihedral angles [252, 251]. B3LYP has also been shown to be quite accurate for vibrational frequencies and zero-point

vibrational energies (ZPVEs) within 2–3% [252, 251, 256]. For instance, the use of B3LYP instead of MP2 for frequency calculations is critical for radical species where MP2 can lead to unexpectedly large errors caused by spin contamination. Another difference between G2M and G2 is the use of coupled-cluster singles plus doubles with perturbative triples (CCSD(T)) energies instead of QCISD(T) energies. From a comparison of the heats of formation and transition state energies for various radical reactions calculated by the QCISD(T), CCSD(T) and MRCI methods, we found that the CCSD(T) results agree better with experimental and most accurate theoretical MRCI data [251, 253]. The G2M approach [251] has now been tested for a great number of chemical reactions and its results have been compared with available experimental data for both the reaction energies and barrier heights. For atomization energies of a test set of 32 first-row compounds, G2M gives the average absolute deviation of $3.7 \, \mathrm{kJ \, mol^{-1}}$ from experiment. The expected accuracy of this method for relative energies of reaction reactants, intermediates, products and transition states in the reactions of ground-state carbon atoms with unsaturated hydrocarbons is 4–$8 \, \mathrm{kJ \, mol^{-1}}$. The preference of G2M over the original G2 method is expected to be particularly significant for open-shell systems with large spin contamination.

For the reactions described in the present review, we used two variants of the G2M methodology. In the first, most extensive scheme, which is applied to the systems with a smaller number of atoms, the energy is calculated as CCSD(T)/6-311 + G(3df, 2p)//B3LYP/6-311G(d, p) + ZPVE[B3LYP/6-311G(d, p)]. This means that geometries and vibrational frequencies were computed at the B3LYP/6-311G(d, p) level and the energies were then refined using single-point CCSD(T)/6-311 + G(3df, 2p) calculations. In the second scheme, G2M(MP2), which is applied for larger systems, the energies were calculated as E[G2M(MP2)] = E[CCSD(T)/6-311G(d, p)] + E[MP2/6-311 + G(3df, 2p)] − E[MP2/6-311G(d, p)] + ZPVE[B3LYP/6-311G(d, p)] + HLC, where HLC $= -5.25 n_\beta - 0.19 n_\alpha$ mHartree. The empirical HLC is only relevant when the number of electron pairs changes during the reaction.

When one investigates a complicated PES with numerous intermediates, transition states and reaction products, the connections between them very often are not obvious from their geometries. In order to clarify these connections and to prove unambiguously that a particular transition state connects two specific intermediates or products, one can use the intrinsic reaction coordinate method [257]. This method allows one to follow the minimal-energy reaction path from a transition state down to the nearest local minima in the forward and reverse directions.

Intersystem crossing (ISC) between PESs with different spin multiplicities might also play a crucial role in chemical dynamics, and in the reactions of the ground state triplet atomic carbon with unsaturated hydrocarbons in particular. The structures on the PES crossing seams open the routes for ISC, that is for the multiplicity change during the reaction course, if the spin–orbit coupling at these geometries is large enough to ensure an efficient ISC process. Therefore, it is important to locate and characterize such intersection points (and hypersurfaces) and to determine their energies. In our calculations, we used the Lagrange multiplier method described by Dunn and Morokuma [258] in order to find minimal energy points on the seam of crossing. In this approach, the wavefunctions for two intersecting electronic states are calculated separately. This gives an advantage of universality; the ISC can be investigated at various levels of theory and the method can work within any *ab-initio* or DFT approximation, from B3LYP to QCISD, CCSD or MRCI, if the energy and

gradient are provided. In the computational algorithm [259], the energies and gradients of two electronic states are taken for the current geometry from *ab-initio* calculations and used to generate the next geometry for which the calculations of energies and gradients for the two states are run again. The iterations continue until a minimum on the line of crossing is located. Similar to the calculations of conventional equilibrium structures, the energies of the minimal points of the line of crossing can be evaluated with the accuracy of $5\text{--}10\,\text{kJ}\,\text{mol}^{-1}$ if one uses accurate *ab-initio* methods such as CCSD(T) or MRCI.

3.2. *Rice–Ramsperger–Kassel–Marcus calculations of reaction rate constants and product branching ratios*

The results of *ab-initio* calculations, for instance molecular structures, energies and vibrational frequencies, can be used to compute rate constants of individual reaction steps and subsequently branching ratios of various reaction products. This opens up an opportunity of a direct comparison between theoretical results and experimental observations. For a unimolecular reaction

$$\text{R}^* \xrightarrow{k} \text{TS}^{\neq} \longrightarrow \text{P}, \tag{1}$$

where R^* is the energized reactant, $\text{TS}^{\neq}$ the activated complex or transition state on the PES, and P the product(s); the microcanonical rate constant $k(E)$ depending on the available internal energy E, can be expressed according to Rice–Ramsperger–Kassel–Marcus (RRKM) theory [260] as

$$k(E) = \frac{\sigma}{h}\frac{W^{\neq}(E - E^{\neq})}{\rho(E)}. \tag{2}$$

Here σ is the symmetry factor, h is the Planck's constant, $W^{\neq}(E - E^{\neq})$ denotes the total number of states of the transition state with an entrance barrier $E^{\neq}$, and $\rho(E)$ represents the density of states of the energized reactant molecule. Since we consider reactions under collision-free conditions such as in molecular clouds or in molecular-beam experiments, the initial thermal distributions are assumed to be at $0\,\text{K}$, so that the initial energy distributions are chemical activation delta functions centred at the critical energy for the respective entrance channels. The $W^{\neq}(E - E^{\neq})$ and $\rho(E)$ values can be evaluated then using the saddle-point method [260] or the Whitten–Rabinovitch approximation [261–263], which generally give similar results.

3.3. *Crossed-beam experiments versus ab-initio calculations*

We would like to note that RRKM calculations alone cannot reveal the actual reaction mechanisms involved. The RRKM theory, for instance, assumes a complete energy randomization in the decomposing intermediate of a bimolecular reaction before the latter fragments. However, crossed-beams studies of $C(^3P_j)$–1,2-butadiene [264], $C(^3P_j)$–CD$_3$CCH [265], $C(^3P_j)$–C$_6$H$_6$, C_6H_5–CH$_3$CCH [266] and the reactions of electronically excited carbon atoms $C(^1D_2)$ with acetylene, ethylene and methyl-acetylene [267, 268] revealed strong discrepancies between the calculated and the experimentally observed product distributions. In addition, PESs cannot predict whether the actual reaction is direct or indirect. On the other hand, electronic structure calculations provide guidance, if, for instance, experimental enthalpies of formation of radical products are missing. Therefore, crossed-beams experiments

and computations of the pertinent PESs are highly complementary to exposing the reaction dynamics of complicated polyatomic reactions comprehensively.

3.4.   *Dynamics calculations*

Dynamics calculations are important to turn the *ab-initio* results into quantities comparable with experiment. Quasiclassical trajectory (QCT) calculations are of particular significance to investigate the effects of the collision energy on the reaction dynamics and to derive scalar and vector properties [269, 270]. These are, for instance, the cross-section as a function of the collision energy, the opacity function, the rovibrational distributions of the products of interest, the translational energy distribution $P(E_T)$, the angular distribution $T(\theta)$ and the differential cross-section as the intensity as a function of angle θ and product centre-of-mass velocity u. These data can be then compared with the experimental results. QCT calculations require an analytical surface, which is fitted using *ab-initio* data, and have been applied very successfully to investigate the reaction dynamics of simple triatomic and tetra-atomic systems [271] such as the reactions of fluorine [272–274], chlorine [275–277], deuterium [278, 279], as well as electronically excited nitrogen ($N(^2D)$) [280, 281], oxygen ($O(^1D)$) [282–284] and ($S(^1D)$) [285, 286] with molecular hydrogen. QCT calculations have been extended also to tetra-atomic systems such as OH–CO [287–289], H–H_2O and OH–H_2 together with their isotopic variants [290–299], CN–H_2 [300] and $O(^1D)$–H_2O [301]. Sayos and co-workers extended a triatomic analytical function to polyatomic systems CH_4–$O(^1D)$ [302–305] and C_2H_6–$O(^1D)$ [306] approximating the methyl (CH_3) and ethyl (C_2H_5) groups as pseudoatoms of masses 15 amu and 29 amu respectively. Recently, Clary [307] utilized a rotating-bond approximation to enable state-to-state quantum scattering calculations on the CH_4–$O(^3P)$ system including explicitly the umbrella modes of the methane reagent and methyl radical product [307].

Considering the reactions of atomic carbon in its ^3P_j ground state, QCT calculations have been performed only for the triatomic $C(^3P_j)$–H_2 system using an accurate *ab-initio* potential surface [308]. This system may be regarded as a prototype for $C(^3P_j)$ reactions with saturated hydrocarbons, because of its simplicity; however, the reaction mechanism with unsaturated hydrocarbons is expected to be distinct, with the addition(s) to the π system being dominant. However, owing to the elaborate PES(s) involved, a theoretical QCT treatment of reactions of atomic carbon with unsaturated hydrocarbons is absent. This can be understood easily, as these surfaces involve highly unsaturated triplet intermediates which can undergo various isomerizations via ring opening and closure and multiple hydrogen migration. This is in strong contrast with the $O(^1D)$–CH_4 and $O(^1D)$–C_2H_6 reactions in which the initial insertion step forms closed-shell methanol and ethanol intermediates respectively. Additionally, the CH_3 group cannot be treated as a spectator or pseudoatom in, for instance, the reactions of carbon atoms with methylacetylene and dimethylacetylene since the hydrogen atom is released from the methyl group (sections 4.1.4 and 4.1.5). This makes QCT calculations extremely challenging. Very recently, Buonomo and Clary [309] investigated the $C(^3P_j)$–C_2H_2 system theoretically using a reduced dimensionality treatment. The experimental finding of an enhanced formation of the cyclic isomer as the collision energy drops seems to be in contradiction to this theoretical study. Here, the linear isomer was found to be the principal reaction product at the whole energy range from 5 to 70 kJ mol^{-1}; c-C_3H was predicted to be formed only at higher energies. However, this approach hardly

treats the experimentally inferred direct reaction dynamics to the c-C$_3$H isomer comprehensively, and more extensive theoretical investigations accounting for a direct pathway are desirable.

4. Results

4.1. *Reaction of atomic carbon with alkynes*

4.1.1. *The C(^3P_j)–C$_2$H(X $^2\Sigma^+$) system*

The reaction of atomic carbon C(^3P_j) with the ethynyl radical C$_2$H(X $^2\Sigma^+$) has only been investigated theoretically [310]. Experimental difficulties to produce high-intensity supersonic beams of carbon atoms and ethynyl radicals simultaneously in a crossed-beam set-up have excluded this important system from being studied experimentally. The doublet C$_3$H PES was calculated at the CCSD(T)/6-311 + G(3df, 2p)/B3LYP/6-311G(d, p) + ZPE(B3LYP/6-311G(d, p) level of theory and depicts two barrierless entrance channels. These pathways proceed via an addition of atomic carbon to the carbon–carbon triple bond of the ethynyl radical and connect the separated reactants to the c-C$_3$H(X $^2B_1$) intermediate (INT1) (pathway 1) and the l-C$_3$H(X $^2\Pi_\Omega$) isomer (INT2) (figure 2). Both intermediates are stabilized by 551.1 kJ mol^{-1} and 544.6 kJ mol^{-1} with respect to the carbon atom plus ethynyl radical and can isomerize via ring opening through a transition state located 114.7 kJ mol^{-1} above INT1. l-C$_3$H(X $^2\Pi_\Omega$) dissociates to l-C$_3$(X $^1\Sigma^+_g$) (p1) without exit barrier. All transition state searches lead to the dissociation products and the minimum search started from l-C$_3$(X $^1\Sigma^+_g$) + H($^2S_{1/2}$) separated by 350 nm gives l-C$_3$H(X $^2\Pi_\Omega$); no minimum of a cyclic tricarbon molecule in a singlet state exists; optimization spontaneously leads to the l-C$_3$(X $^1\Sigma^+_g$) isomer. On the other hand,
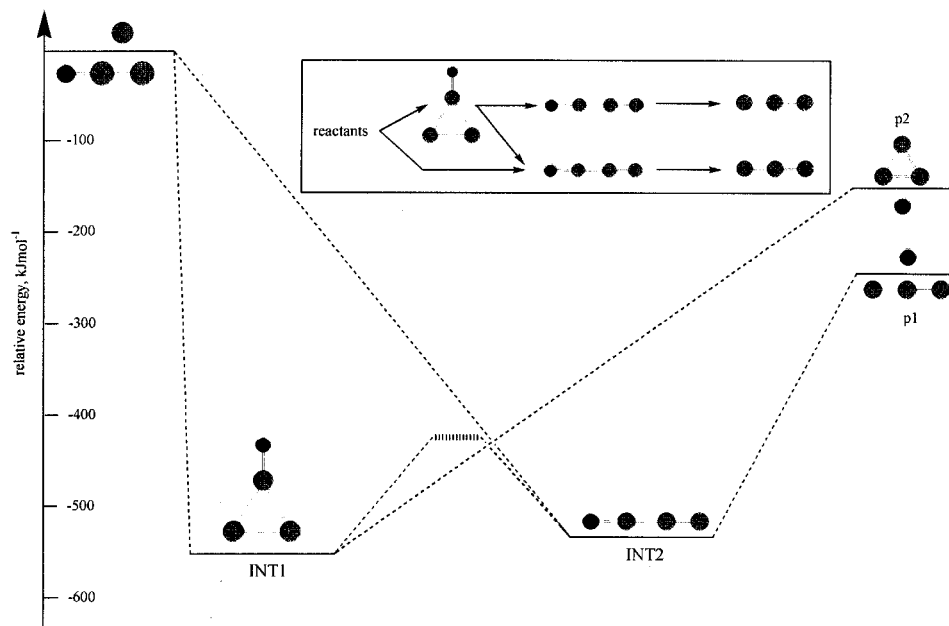

Figure 2. Simplified PESs of the reaction of ground-state atomic carbon with the ethynyl radical. Carbon atoms are denoted in black, and hydrogen atoms in grey.

cyclic tricarbon is stable in its triplet A_1' state as a 2π-electron aromatic molecule with D_{3h} symmetry in a sense analogous to the c-$C_3H_3^+$ structure. This c-$C_3(X\,^3A_2')$ structure p2 lies only 82.0 kJ mol^{-1} higher in energy than l-$C_3(X\,^1\Sigma_g^+)$. There is also no exit barrier for the dissociation of INT1 to c-$C_3(X\,^3A_2')$ and atomic hydrogen. Our calculations depicted further that no reaction path connecting INT1 to l-$C_3(X\,^1\Sigma_g^+)$ + H($^2S_{1/2}$) exists; likewise C(^3P_j) does not insert into the hydrogen–carbon σ bond of the ethynyl radical. The overall reaction enthalpies to form l-$C_3(X\,^1\Sigma_g^+)$ + H($^2S_{1/2}$) (channel 1) and c-$C_3(X\,^3A_1')$ + H($^2S_{1/2}$) (channel 2) were calculated to be -244.6 kJ mol^{-1} and -162.2 kJ mol^{-1} respectively. The data of channel 1 are close to an experimental value of -234.6 kJ mol^{-1} (table 1). An alternative reaction pathway to form $C_2(X\,^1\Sigma_g^+)$ + CH($X\,^2\Pi_\Omega$) via a homolytic cleavage of the carbon–carbon bond of INT2 is endoergic by 159.2 kJ mol^{-1} and, therefore, closed. Summarizing, the reaction of atomic carbon C(^3P_j) with the ethynyl radical $C_2H(X\,^2\Sigma^+)$ is expected to form the l-$C_3(X\,^1\Sigma_g^+)$ + H($^2S_{1/2}$) and c-$C_3(X\,^3A_1')$ + H($^2S_{1/2}$) products in exoergic reactions.

Future crossed-beams studies should focus on the collision energy and hence impact-parameter-dependent reaction dynamics to form both tricarbon isomers. These information could be extracted from the centre-of-mass angular distributions and might resolve the initial formation of INT1 versus INT2. The experiments could unravel, if direct reaction dynamics similar to the C(^3P_j)–$C_2H_2(X\,^1\Sigma_g^+)$ system (section 4.1.2) are also involved. This is expected to have important consequences for the lifetimes of the intermediates. For instance, INT1 can isomerize to INT2 via two microchannels (figure 2) to form two distinct intermediates in which the new carbon atom is either located at the central (top) or terminal (bottom) position. Since INT2 can also be formed from the reactants, three microchannels, possibly involving different impact parameters, can synthesize INT2; this could result in distinct lifetimes of the intermediates and hence in strongly different reaction dynamics of each microchannel.

4.1.2. *The C(^3P_j)–$C_2H_2(X\,^1\Sigma_g^+)$ system*

Bimolecular collisions of carbon atoms C(^3P_j) with acetylene $C_2H_2(X\,^1\Sigma_g^+)$ represent prototype encounters of atomic carbon with the simplest closed-shell alkyne. Because of this importance, the C(^3P_j)–$C_2H_2(X\,^1\Sigma_g^+)$ system has been investigated both theoretically [309, 312–314] and experimentally in crossed-beams experiments [311, 313, 315]. The computations reveal that similar to the C(^3P_j)–$C_2H(X\,^2\Sigma^+)$ system, atomic carbon reacts solely via addition to the carbon–carbon triple bond of the acetylene molecule. Two reaction pathways were located on the

Table 1. Reaction enthalpies of various exit channels of the C(^3P_j) + $C_2H(X\,^2\Sigma^+)$ reaction. Enthalpies of formations of reactants and products are taken from [311].

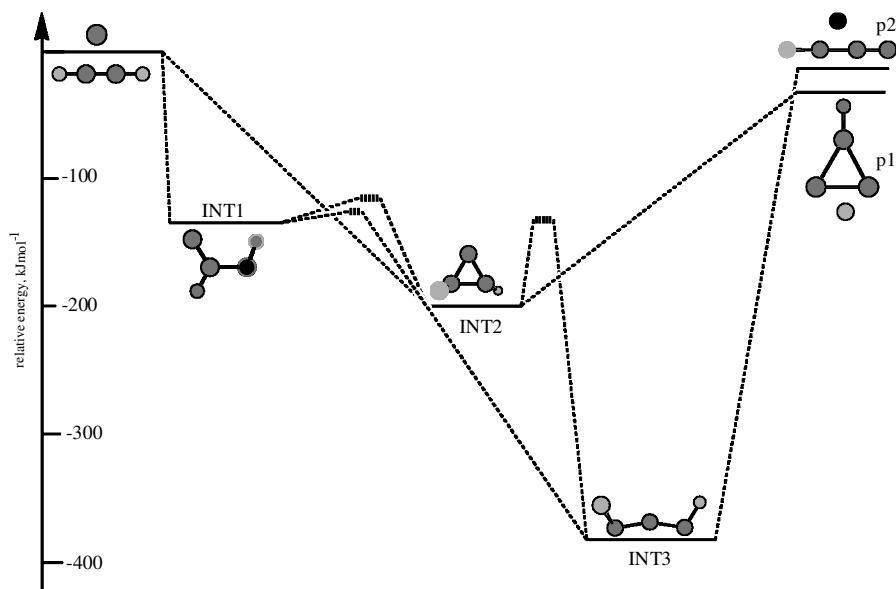| Products	Reaction enthalpy (kJ mol^{-1})
l-$C_3(X\,^1\Sigma_g^+)$ + H($^2S_{1/2}$)	-234.6
c-$C_3(X\,^3A_2')$ + H($^2S_{1/2}$)	-162.2
$C_2(X\,^1\Sigma_g^+)$ + CH($X\,^2\Pi_\Omega$)	$+159.2$

Figure 3. Simplified PESs of the reaction of ground-state atomic carbon with acetylene. Carbon atoms are denoted in black, and hydrogen atoms in grey.

triplet surface which can lead to the formation of trans propenediylidene (CHCCH(X^3A''); INT1) (addition to one carbon atom) and to cyclopropenylidene (c-C_3H_2(a ^3A); INT2) (figure 3). Both isomers are stabilized by 122–137 kJ mol^{-1} and 190–216 kJ mol^{-1} with respect to the reactants and are connected via ring opening or closure through a transition state located 3–4 kJ mol^{-1} above INT1. The latter can undergo also a [2, 3]-H migration to triplet propargylene (HCCCH(X^3B), INT3) via a barrier of 0.1–11 kJ mol^{-1}; propargylene presents the global minimum of the triplet surface and is bound by 352–388 kJ mol^{-1} with respect to the reactants. INT2 might isomerize via ring opening to INT3 as well. Both intermediates INT2 and INT3 decay without an additional exit barrier via emission of atomic hydrogen to form c-C_3H(X^2B_1) (p1) and l-C_3H($X^2\Pi_\Omega$) (p2); the overall reaction enthalpies were calculated to be -8.6 kJ mol^{-1} and -1.5 kJ mol^{-1} respectively (table 2).

Table 2. Reaction enthalpies of various exit channels of the $C(^3P_j) + C_2H_2(X^1\Sigma_g^+)$ reaction. Enthalpies of formations of reactants and products are taken from [311].

Products	Reaction enthalpy (kJ mol^{-1})
c-C_3H(X^2B_1) + $H(^2S_{1/2})$	-8.6
l-C_3H($X^2\Pi_\Omega$) + $H(^2S_{1/2})$	-1.5
$C_3(X^1\Sigma_g^+)$ + $H_2(X^1\Sigma_g^+)$	-123.3
$CH_2(X^3B_1)$ + $C_2(X^1\Sigma_g^+)$	$+280.8$
$C_2H(X^2\Sigma^+)$ + $CH(X^2\Pi_\Omega)$	$+206.8$

The crossed-beams experiments verified the existence of this atomic carbon versus hydrogen exchange. Reactive scattering signal was observed at a mass-to-charge ratio of 37 (C_3H^+). A forward-convolution fitting of the data yielded further centre-of-mass angular flux distributions which were decreasingly forward scattered with respect to the carbon beam as the collision energy rises from 8.8 to 28.0 kJ mol^{-1} and were isotropic at 45.0 kJ mol^{-1}. It was inferred that the reaction dynamics involve at least two microchannels which were initiated by a barrierless addition of C(^3P_j) either to one acetylenic carbon, yielding INT1, or to two carbon atoms to form INT2. Propenediylidene was proposed to follow a [2, 3]-H migration to INT3, leading ultimately to l-C_3H (X $^2\Pi_\Omega$) plus atomic hydrogen via a homolytic carbon–hydrogen bond rupture via a symmetric exit transition state. Direct stripping dynamics were suggested to contribute to the forward-scattered second microchannel giving the C_{2v} symmetric c-C_3H(X $^2B_2$) isomer together with atomic hydrogen. This pathway was quenched as the collision energy increases. Note that the result of an increased formation of c-C_3H(X $^2B_2$) as the collision energy drops seems to be in contradiction to a recent quantum-mechanical study of this [316]. The linear isomer was found to be the principal reaction product; the cyclic isomer was proposed to be synthesized solely at higher energies. However, this approach does not account for the experimentally inferred direct reaction dynamics to form the c-C_3H isomer; therefore additional experimental and theoretical investigations on this reaction are desirable to solve these discrepancies. In particular, INT3 intermediates with distinct lifetimes have to been taken into serious consideration [225]. Similar to the reaction of carbon atoms with the ethynyl radical, different formation routes of the intermediates involved can translate into a distinct energy randomization. For instance, generation of INT3 can proceed via INT1 → INT3, INT1 INT2 → INT3 and INT2 → INT3 through three different pathways. Denoting the incorporated carbon atom in bold, this might lead to H**C**CCH, HC**C**CH and HCC**C**H. Depending on the initial impact parameter and hence rovibratational excitation of the INT3 intermediates, distinct lifetimes might result. These unsolved problems should be tackled further substituting C_2HD(X $^1\Sigma^+$) for the C_2H_2 (X $^1\Sigma_g^+$) reactant, photo-ionization of the reaction products and performing the experiment with ^{13}C.

We discuss now briefly additional reaction pathways besides the atomic hydrogen loss. The contemporary experimental assignment of the exoergic, formally spin-forbidden C_3(X $^1\Sigma_g^+$) + H_2(X $^1\Sigma_g^+$) channel, which has a branching ratio of 30–40%, demonstrated convincingly that the mechanism to form C_3H isomers is indeed more complex [227, 317]. Electronic structure calculations predicted that intersystem crossing of triplet INT3 to the singlet surface is facile [318]. The singlet propargylene intermediate can lose molecular hydrogen via a five-membered cyclic transition state or isomerizes via a [1, 3]-H shift to form singlet vinylidenecarbene prior to a molecular hydrogen ejection to form the tricarbon molecule. Hence, singlet propargylene and vinylidenecarbene can also decompose barrierless atomic hydrogen elimination to the l-C_3H isomer. In addition, singlet propargylene can ring close to singlet cyclopropenylidene, which can lose a hydrogen atom, yielding c-C_3H. Therefore three distinct pathways might actually form l-C_3H; as discussed above, direct dynamics or a pathway via the triplet–singlet ISC and singlet c-C_3H_2 may account for the c-C_3H isomer at lower collision energies. Note that a crossed-beams investigation of the C(^3P_j)–C_2H_2(X $^1\Sigma_g^+$) system at collision energies higher than 200 kJ mol^{-1} opened also the endoergic CH(X $^2\Pi_\Omega$) + C_2H(X $^2\Sigma^+$) channel [319]. However, in molecular clouds, both endoergic reaction pathways to form

$CH_2(X\,^3B_1) + C_2(X\,^1\Sigma_g^+)$ and $C_2H(X\,^2\Sigma^+) + CH(X\,^2\Pi_\Omega)$ are thermodynamically forbidden.

4.1.3. *The $C(^3P_j)$–$C_3H_3(X\,^2B_1)$ system*

The reaction of atomic carbon $C(^3P_j)$ with the propargyl radical $C_3H_3(X\,^2B_1)$ represents the only atom–radical system that has been investigated theoretically [320] and in a crossed-beams experiment at a collision energy of $42.0\,\mathrm{kJ\,mol^{-1}}$ [321]. Similar to the reactions with the ethynyl radical and acetylene, the carbon atom was found to add in a barrierless way either to two carbon atoms of the carbon–carbon triple bond, forming the cyclic intermediate INT1 (pathway 1), or to the terminal acetylenic carbon atom to give INT2 (pathway 2) (figure 4). The latter pathway deserves particular attention. The computations show that INT2 is stabilized by $328.4\,\mathrm{kJ\,mol^{-1}}$ with respect to the separated reactants; however, the barrier for a hydrogen migration to INT3 is very low, only 0.4–$1.2\,\mathrm{kJ\,mol^{-1}}$ and disappears when zero-point-energy corrections are used [320]. Therefore, INT2 is probably not a stable intermediate, and pathway 2 proceeds by an addition of the carbon atom to form INT2 followed by a barrierless hydrogen shift to give INT3. Both INT1 and INT3 lie $426.1\,\mathrm{kJ\,mol^{-1}}$ and $549.7\,\mathrm{kJ\,mol^{-1}}$ below the reactants and are connected via ring opening through a transition state located $88.8\,\mathrm{kJ\,mol^{-1}}$ above INT1. The experimentally inferred indirect reaction dynamics are supported by the deep potential energy well of n-C_4H_3 (INT3). INT3 was found to decompose via atomic hydrogen loss forming the diacetylene molecule $C_4H_2(X\,^1\Sigma_g^+)$ (p1) through a tight exit transition state located about $30\,\mathrm{kJ\,mol^{-1}}$ above the products. RRKM calculations demonstrate that about 8% of the diacetylene is formed via a hydrogen shift in INT3 to the i-C_4H_3 isomer (INT4) prior to dissociation of the latter. The theory predicts further that two minor exoergic pathways of less than a few per cent might form the butatrienylidene radical ($C_4H(X\,^2\Sigma^+)$) (p2) and acetylene ($C_2H_2(X\,^1\Sigma_g^+)$)
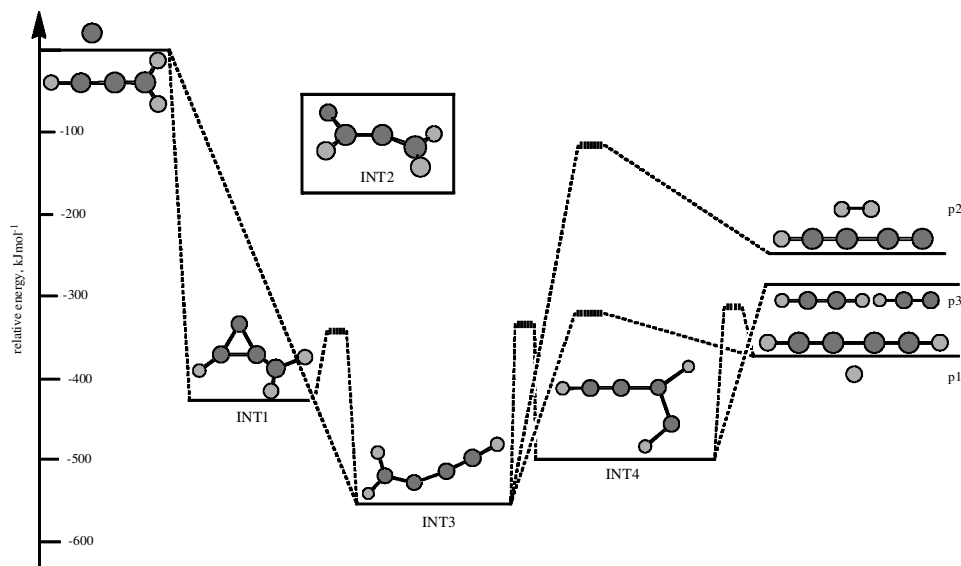

Figure 4. Simplified PESs of the reaction of ground-state atomic carbon with the propargyl radical. Carbon atoms are denoted in black, and hydrogen atoms in grey.

Table 3. Reaction enthalpies of various exit channels of the $C(^3P_j) + C_3H_3(X\,^2B_1)$ reaction. Enthalpies of formations of reactants and products are taken from [311].

Products	Reaction enthalpy (kJ mol^{-1})
$C_4H_2(X\,^1\Sigma_g^+) + H(^2S_{1/2})$	-373.7
$C_4H(X\,^2\Sigma^+) + H_2(X\,^1\Sigma_g^+)$	-233.4
$C_2H_3(X\,^2A') + C_2(X\,^1\Sigma_g^+)$	$+81.0$
$C_3H_2(X\,^1A_1) + CH(X\,^2\Pi_\Omega)$	$+38.4$
$HCCCH(X\,^3B) + CH(X\,^2\Pi_\Omega)$	$+94.5$
$H_2CCC(X\,^1A_1) + CH(X\,^2\Pi_\Omega)$	$+101.4$
$CH_3(X\,^2A_2'') + C_3(X\,^1\Sigma_g^+)$	-88.6
$c\text{-}C_3H(X\,^2B_1) + CH_2(X\,^3B_1)$	$+47.4$
$l\text{-}C_3H(X\,^2\Pi_\Omega) + CH_2(X\,^3B_1)$	$+54.4$
$C_2H_2(X\,^1\Sigma_g^+) + C_2H(X\,^2\Sigma^+)$	-273.0

(p3) through a decomposition of INT4 via molecular hydrogen and ethynyl $C_2H(X\,^2\Sigma^+)$ loss respectively (table 3). Although the formation of $CH_3(X\,^2A_2'') + C_3(X\,^1\Sigma_g^+)$ is exothermic by 88.6 kJ mol^{-1}, none of the most important intermediates involved connects to these products; therefore tricarbon and the methyl radical are unlikely to be formed in the bimolecular reaction of atomic carbon with propargyl. Note that all endoergic pathways as compiled in table 3 are also closed in cold molecular clouds.

4.1.4. *The $C(^3P_j)$–$CH_3CCH(X\,^1A_1)$ system*

The underlying PES and reaction dynamics of the $C(^3P_j)$–CH_3CCH system depict pronounced similarities to but also distinct differences from the reaction of atomic carbon with acetylene. Firstly, the reaction of methylacetylene proceeds via indirect scattering dynamics and is initiated by a barrierless addition of $C(^3P_j)$ to the carbon–carbon triple bond to either one or both carbon atoms (figure 5) [322–324]. Reactions with large impact parameters yield a triplet *trans*-methylpropene-1-diylidene intermediate (INT1) whereas, to a minor amount, the formation of a triplet methylcyclopropenylidene intermediate INT2 is governed by smaller impact parameters. Note that INT1 can exist in either a *trans* or *cis* form which can isomerize rapidly. The preferential attack of the C(1) atom of the methylacetylene molecule is supported by an enhanced electron density of the C(1) atom ($-0.14e$) compared with that of the C(2) atom ($-0.11e$) owing to the π-group orbitals of the methyl substituent and the screening effect of the CH_3 group (sterical hindrance), thus reducing the cone of acceptance at C(2). INT1 and INT2 are stabilized by 137 kJ mol^{-1} and 221 kJ mol^{-1} and are connected via a barrier of about 18 kJ mol^{-1}. Similar to the propenediylidene and cyclopropenylidene intermediates in the $C(^3P_j)$–C_2H_2 system, INT1 and INT2 were found to undergo also hydrogen shift and ring opening respectively to form the triplet methylpropargylene isomer INT3. The barriers involved are located 0.8 kJ mol^{-1} and 61–65 kJ mol^{-1} above INT1 and INT2 respectively. Methylpropargylene (INT3) resides in a deep potential energy well of 374 kJ mol^{-1} and decomposes through a hydrogen atom loss via a tight transition state located 18–24 kJ mol^{-1} above the products giving the $n\text{-}C_4H_3(X\,^2A')$
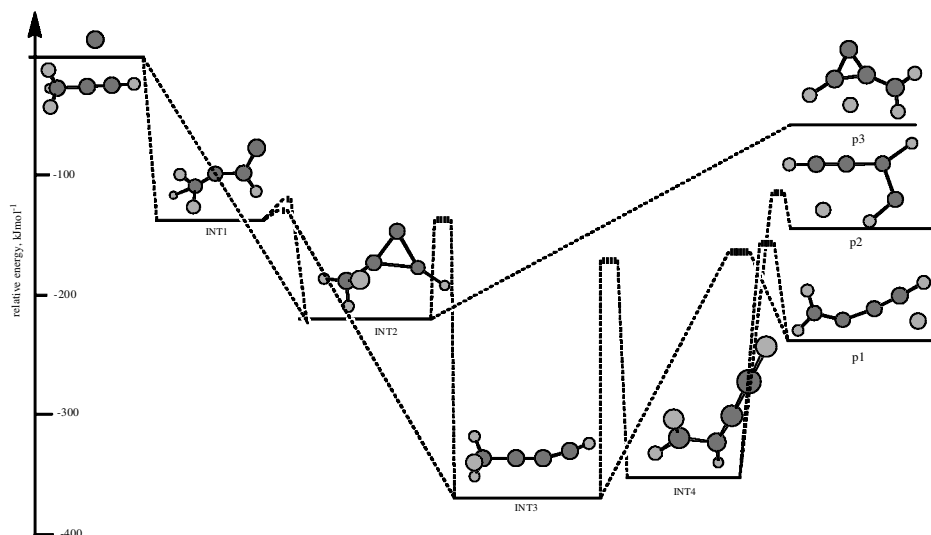
Figure 5. Simplified PESs of the reaction of ground-state atomic carbon with methylacetylene. Carbon atoms are denoted in black, and hydrogen atoms in grey.

product p1. RRKM calculations suggest further that the formation of a second C_4H_3 chain isomer p2 via INT3 and INT4 is less important (about 1%). Note that, at lower collision energies, a cyclic C_4H_3 isomer (p3) might also be formed via INT2 in which the energy randomization is incomplete [265].

Finally, we would like to discuss alternative exit channels besides an atomic hydrogen loss pathway (table 4). Although the formation of diacetylene in its ground

Table 4. Reaction enthalpies of various exit channels of the $C(^3P_j) + CH_3CCH(X\,^1A_1)$ reaction. Enthalpies of formations of reactants and products are taken from [311].

Products	Reaction enthalpy $(kJ\,mol^{-1})$
$n\text{-}C_4H_3(X\,^2A') + H(^2S_{1/2})$	-174.8
$C_4H_2(X\,^1\Sigma_g^+) + H_2(X\,^1\Sigma_g^+)$	-438.1
$C_4H_2(a\,^3\Pi_g) + H_2(X\,^1\Sigma_g^+)$	-52.6
$C_2H_4(X\,^1A_{1g}) + C_2(X\,^1\Sigma_g^+)$	-11.9
$C_2H_4(X\,^1A_{1g}) + C_2(a\,^3\Pi_u)$	-3.9
$C_3H_3(X\,^2B_1) + CH(X\,^2\Pi_\Omega)$	$+31.0$
$CH_4(X\,^1A_1) + C_3(X\,^1\Sigma_g^+)$	-156.9
$CH_4(X\,^1A_1) + C_3(a\,^3\Pi_u)$	$+45.6$
$C_2H_3(X\,^2A') + C_2H(X\,^2\Sigma^+)$	-47.0
$C_3H_2(X\,^1A_1) + CH_2(X\,^3B_1)$	-15.7
$HCCCH(X\,^3B) + CH_2(a\,^1A_1)$	$+40.3$
$H_2CCC(X\,^1A_1) + CH_2(X\,^3B_1)$	$+47.3$
$c\text{-}C_3H(X\,^2B_1) + CH_3(X\,^2A_2'')$	-38.4
$l\text{-}C_3H(X\,^2\Pi_\Omega) + CH_3(X\,^2A_2'')$	-31.3
$C_2H_2(X\,^1\Sigma_g^+) + C_2H_2(X\,^1\Sigma_g^+)$	-448.7
$C_2H_2(X\,^1\Sigma_g^+) + C_2H_2(a\,^3\Pi_u)$	-46.5

state ($X\,^1\Sigma_g^+$) and excited triplet state (a $^3\Pi_g$) is exothermic, no experimental evidence of a molecular hydrogen elimination was found. This has been supported by the electronic structure calculations; here, INT3 is the sole candidate to form C_4H_2(a $^3\Pi_g$) + H_2 with total reaction exothermicity of 52.6 kJ mol^{-1}, but a barrier for the H_2 loss is expected to be high. For instance, the transition state for the H_2 elimination from a close analogue of INT3, the CCCCH$_3$ radical, lies 110 kJ mol^{-1} above the CCCCH + H_2 products [284]. Likewise, the C_2H_4($X\,^1A_{1g}$) + C_2($X\,^1\Sigma_g^+$) and C_2H_4($X\,^1A_{1g}$) + C_2(a $^3\Pi_u$) pathways are closed as no intermediate involved connects to ethylene and dicarbon. Similar arguments support the fact that the formation of the three C_3H_2 isomers and the C_3H_3($X\,^2B_1$) + CH($X\,^2\Pi_\Omega$), C_2H_2($X\,^1\Sigma_g^+$) + C_2H_2($X\,^1\Sigma_g^+$) and C_2H_2($X\,^1\Sigma_g^+$) + C_2H_2(a $^3\Pi_u$) pathways either are too endoergic or require C_4H_4 intermediates which are not accessible on the PES involved. However, the l-C_3H($X\,^2\Pi_\Omega$) + CH_3($X\,^2A_2''$) and c-C_3H($X\,^2B_1$) + CH_3($X\,^2A_2''$) channels probably present minor pathways via a methyl group loss from INT2 and INT3 respectively of a few per cent at most. Unfortunately, because of the inherent background in the detector of the crossed-beams experiment from fragmentation of the methylacetylene reactant, both pathways have not yet been verified experimentally. The C_2H_3($X\,^2A'$) + C_2H($X\,^2\Sigma^+$) channel is expected to be only of minor importance since RRKM calculations show that INT4, which is required to undergo a homolytic carbon–carbon bond cleavage to firm ethynyl and vinyl, plays only a less important role (less than 1%) even in the formation of p2. Finally, the spin-forbidden pathway to form CH_4($X\,^1A_1$) + C_3($X\,^1\Sigma_g^+$) has to be addressed. Formally, this would correspond to an elimination of methane via a five-membered cyclic transition state from a hypothetical singlet intermediate INT3 which is similar to the molecular hydrogen elimination in the C(^3P_j) + C_2H_2 reaction. The CH_4 elimination would require an ISC from triplet INT3 to the singlet surface; this is currently under investigation.

4.1.5.   *The C(^3P_j)–CH$_3$CCCH$_3$(X $^1A_{1g}$) system*

The reaction between atomic carbon and dimethylacetylene has also no entrance barrier [325]. It follows indirect scattering dynamics through a bound intermediate. C(^3P_j) attacks the π system of the dimethylacetylene molecule to form a dimethylcyclopropenylidene intermediate (INT2; -225.1 kJ mol^{-1}) either in one step via an addition to C(1) and C(2) atoms of the acetylenic bond (small impact parameters) or through an addition to only one carbon atom to give short-lived *cis* and *trans* dimethylpropenediylidene intermediates (INT1; -131.8 to -123.8 kJ mol^{-1}) via larger impact parameters followed by a ring closure (figure 6). The cyclic intermediate INT2 ring opens via a barrier of 64.4 kJ mol^{-1} to the dimethyl-propargylene (INT3) in which the carbon atoms depict a linear arrangement. This species is stabilized by 374.0 kJ mol^{-1} with respect to the separated reactants and fragments to atomic hydrogen and a linear 1-methylbutatrienyl radical H_2CCCCCH$_3$ ($X\,^2A''$), via a tight exit transition state located about 18 kJ mol^{-1} above the separated products. The experimentally determined exothermicity of 190 ± 25 kJ mol^{-1} is in strong agreement with the calculated data of 181.2 kJ mol^{-1}, (table 5). Compared with the reaction with methylacetylene, the substitution of a hydrogen atom by a methyl group increases the lifetime of the decomposing intermediate INT3, and the reaction changes from an osculating complex (CH$_3$CCH) to a long-lived intermediate (CH$_3$CCCH$_3$).
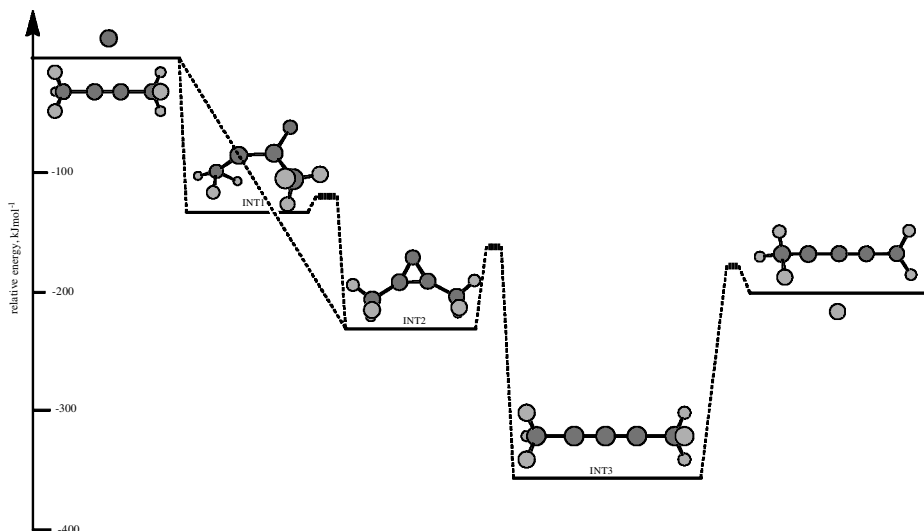
Figure 6. Simplified PESs of the reaction of ground-state atomic carbon with dimethylacetylene. Carbon atoms are denoted in black, and hydrogen atoms in grey.

Table 5. Reaction enthalpies of various exit channels of the reaction $C(^3P_j) + CH_3CCCH_3(X\,^1A_{1g})$. Enthalpies of formations of reactants and products are taken from [311].

Products	Reaction enthalpy $(kJ\,mol^{-1})$
$CH_3CCCCH_2(X\,^2A'') + H(^2S_{1/2})$	-181.2
$CH_3CCCCH(X\,^1A_1) + H_2(X\,^1\Sigma_g^+)$	-448.2
$C_2(X\,^1\Sigma_g^+) + C_3H_6(X\,^1A')$	-3.7
$C_2(a\,^3\Pi_u) + C_3H_6(X\,^1A')$	$+4.3$
$CH(X\,^2\Pi_\Omega) + CH_3CCCH_2(X\,^2A'')$	$+50.6$
$C_3(X\,^1\Sigma_g^+) + C_2H_6(X\,^1A_{1g})$	-125.0
$C_3(a\,^3\Pi_u) + C_2H_6(X\,^1A_{1g})$	$+75.0$
$C_2H(X\,^2\Sigma^+) + C_3H_5(X\,^2B_1)$	-213.8
$CH_2(X\,^3B_1) + HCCC_2H_3(X\,^1A')$	-180.4
$c\text{-}C_3H(X\,^2B_1) + C_2H_5\ (X\,^2A')$	-26.1
$l\text{-}C_3H(X\,^2\Pi_\Omega) + C_2H_5(X\,^2A')$	-19.0
$C_2H_2(X\,^1\Sigma_g^+) + CH_3CCH(X\,^1A_1)$	-449.7
$C_2H_2(a\,^3\Pi_u) + CH_3CCH(X\,^1A_1)$	-47.5
$C_2H_2(X\,^1\Sigma_g^+) + H_2CCCH_2(X\,^1A_1)$	-444.6
$C_2H_2(a\,^3\Pi_u) + H_2CCCH_2(X\,^1A_1)$	-42.2
$CH_3(X\,^2A_2'') + n\text{-}C_4H_3(X\,^2A')$	-206.8
$c\text{-}C_3H_2(X\,^1A_1) + C_2H_4(X\,^1A_{1g})$	-309.3
$HCCCH(X\,^3B) + C_2H_4(X\,^1A_{1g})$	-253.3
$H_2CCC(X\,^1A_1) + C_2H_4(X\,^1A_{1g})$	-246.3
$C_2H_3(X\,^2A') + C_3H_3(X\,^2B_1)$	-223.8
$CH_4(X\,^1A_1) + C_4H_2(X\,^1\Sigma_g^+)$	-472.7
$CH_4(X\,^1A_1) + C_4H_2(a\,^3\Pi_g)$	-87.2

As is obvious from table 5, additional reaction pathways might be open as well. First, a molecular hydrogen elimination to form $C_5H_4(X^1\Sigma^+)$ can be excluded as the TOF spectra at mass-to-charge ratios of 64 and 65 are identical; this indicates strongly that signal at $m/e = 64$ originates from cracking of $m/e = 65$ in the electron impact ionizer. Based on the triplet PES, only a methyl group loss from the intermediates involved to form the $CCCCH_3$ and $c\text{-}C_3CH_3$ products might represent an additional pathway. These C_4H_3 isomers are energetically less stable than the $n\text{-}C_4H_3(X^2A')$ structure, and the reaction enthalpies are calculated to be $-36.8\,kJ\,mol^{-1}$ and $-62.3\,kJ\,mol^{-1}$ respectively [290, 326]. Finally, a potential ISC is addressed briefly. Similar to the propargylene radical, the dimethylpropargylene might undergo ISC to the singlet surface followed by an elimination of ethane via a five-membered cyclic transition state. This pathway would form also the linear tricarbon molecule; detailed calculations are in progress.

4.2. *Reactions of atomic carbon with alkenes and cummulenes*
4.2.1. *The $C(^3P_j)$–$C_2H_3(X^2A')$ system*

Only restricted experimental data on the atom–radical reaction of atomic carbon $C(^3P_j)$ with the vinyl radical $C_2H_3(X^2A')$ are available [327]. These investigations demonstrated clearly the existence of an atomic carbon versus hydrogen atom exchange. However, likely reaction products and mechanisms involved are inferred predominantly from theoretical investigations [328, 329]. In strong analogy to the reaction of atomic carbon with alkynes and their radicals, $C(^3P_j)$, adds in a barrierless manner to the π bond (figure 7). Two reaction pathways have been identified: the formation of a cyclic intermediate INT1 and a chain isomer INT2. The two structures lie $468.4\,kJ\,mol^{-1}$ and $440.0\,kJ\,mol^{-1}$ below the energy of the
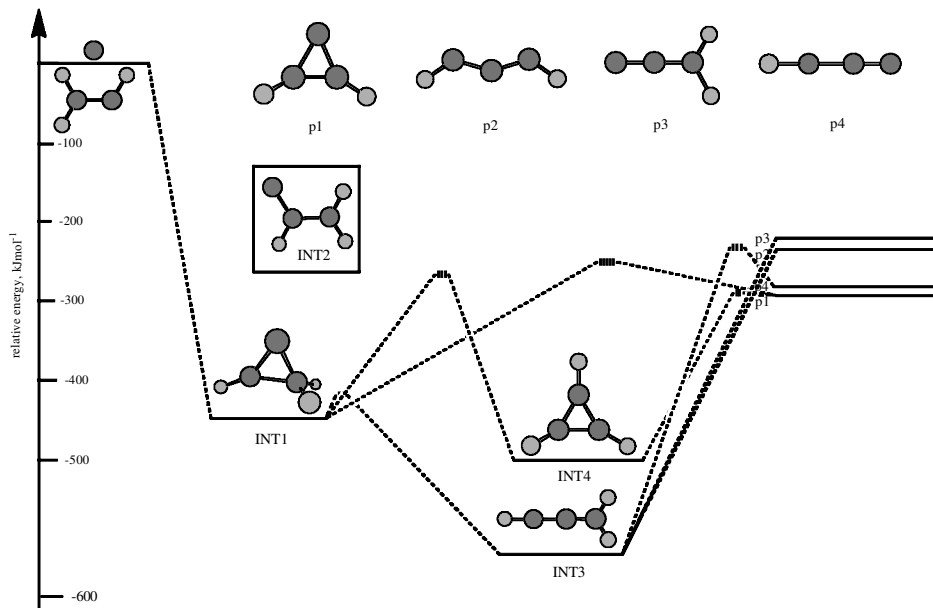

Figure 7. Simplified PESs of the reaction of ground-state atomic carbon with the vinyl radical. Carbon atoms are denoted in black, and hydrogen atoms in grey.

reactants. Similar to the $C(^3P_j)$–$C_3H_3(X\,^2B_1)$ system (figure 4), the barrier for hydrogen migration in INT2 is very low and vanishes when zero-point-energy corrections are used. Therefore, INT2 is probably not a stable intermediate but rather rearranges via a hydrogen shift to the propargyl radical INT3. The latter is the global minimum of the PES, resides in a deep potential energy well of $636.5\,kJ\,mol^{-1}$ and can be formed also via ring opening of INT2 via a barrier of only $39.8\,kJ\,mol^{-1}$. To a minor amount, INT2 can undergo a hydrogen shift to the cyclopropenyl radical INT4; the barrier involved is significantly higher ($+211.6\,kJ\,mol^{-1}$) than for the ring opening. We would like to stress, however, that both pathways that yield INT3 via INT1 and INT2 form distinct propargyl intermediates. Denoting the attacking carbon atom in bold, pathway 1 would lead to a **HC**CCH$_2$ intermediate, whereas pathway 2 would locate the carbon atom at HC**C**CH$_2$. Trajectories with large impact parameters probably provide **HC**CCH$_2$, whereas small impact parameters are expected to form the centre-labelled structure HC**C**CH$_2$. Owing to angular momentum conservation, both pathways are expected to lead to distinct rotational excitation of the final products; further, the lifetimes of **HC**CCH$_2$ and HC**C**CH$_2$ might be also different. However, under the assumption that energy randomization is complete, RRKM calculations predict that the intermediates decompose predominantly via hydrogen atom loss to propargylene (HCCCH(X$\,^3$B); p2; 78–82%), cyclopropenylidene (c-C$_3$H$_2$(X$\,^1$A$_1$); p1; 6–7%), vinylidenecarbene (H$_2$CCC(X$\,^1$A$_1$); p3; 4–8%), and about 5% via molecular hydrogen loss to the l-C$_3$H isomer (p4) (table 6). In addition, a homolytic cleavage of the carbon–carbon bond in INT3 was found to form C$_2$H$_2$(X$\,^1\Sigma_g^+$) + CH(X$\,^2\Pi_\Omega$) (1–2%). Comparing the exothermicity of this pathway with those of the CH$_3$(X$\,^2$A$_2''$) + C$_2$(X$\,^1\Sigma_g^+$) and C$_2$H(X$\,^2\Sigma^+$) + CH$_2$(X$\,^3$B$_1$) products, both latter channels can be safely excluded.

4.2.2. *The $C(^3P_j)$–$C_2H_4(X\,^1A_{1g})$ system*

The reaction of atomic carbon with ethylene is also barrierless and initiated by an addition of the carbon atom to the carbon–carbon double bond to form a triplet cyclopropylidene intermediate INT1 (figure 8) [186, 330]. The latter is stabilized by $216.6\,kJ\,mol^{-1}$ relative to the reactants and isomerizes via ring opening through a barrier of $56.1\,kJ\,mol^{-1}$ to triplet allene INT2. A competing hydrogen shift from

Table 6. Reaction enthalpies of various exit channels of the reaction $C(^3P_j)$ + $C_2H_3(X\,^2A')$. Enthalpies of formations of reactants and products are taken from [311].

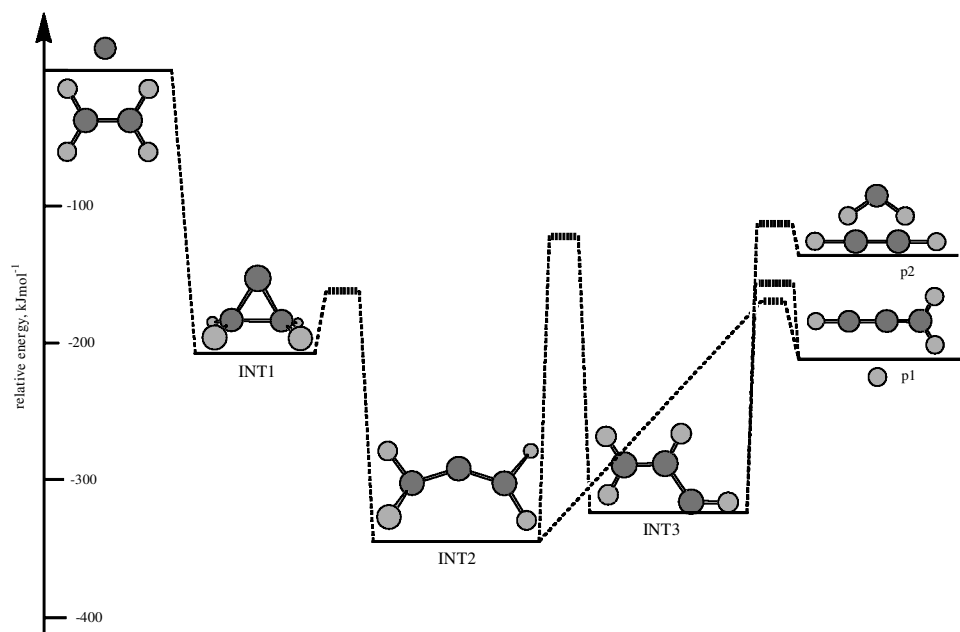| Products	Reaction enthalpy $(kJ\,mol^{-1})$
c-C$_3$H$_2$(X$\,^1$A$_1$) + H(^{2}S$_{1/2}$)	−291.2
HCCCH(X$\,^3$B) + H(^{2}S$_{1/2}$)	−238.8
H$_2$CCC(X$\,^1$A$_1$) + H(^{2}S$_{1/2}$)	−234.6
c-C$_3$H(X$\,^2$B$_1$) + H$_2$(X$\,^1\Sigma_g^+$)	−299.0
l-C$_3$H(X$\,^2\Pi_\Omega$) + H$_2$(X$\,^1\Sigma_g^+$)	−291.9
CH$_3$(X$\,^2$A$_2''$) + C$_2$(X$\,^1\Sigma_g^+$)	−30.9
C$_2$H$_2$(X$\,^1\Sigma_g^+$) + CH(X$\,^2\Pi_\Omega$)	−194.8
C$_2$H(X$\,^2\Sigma^+$) + CH$_2$(X$\,^3$B$_1$)	−73.3

Figure 8. Simplified PESs of the reaction of ground-state atomic carbon with ethylene. Carbon atoms are denoted in black, and hydrogen atoms in grey.

INT1 to a triplet cyclopropene intermediate is unfavourable because of a significant barrier. The triplet allene intermediate resides in a deep potential energy well of $343.2 \, \text{kJ mol}^{-1}$ and decomposes predominantly via a tight exit transition state located $18.9 \, \text{kJ mol}^{-1}$ above the separated products by atomic hydrogen loss to form the propargyl radical p1. The experimental data strongly support the existence of an exit barrier since the centre-of-mass translation energy distribution peaks at $28–60 \, \text{kJ mol}^{-1}$. The reaction with ethylene shows also a second microchannel to form propargyl radicals via direct scattering dynamics; this contribution is quenched as the collision energy rises. In addition, RRKM calculations suggest that a minor fraction of triplet allene INT2 of about 7% rearranges via a hydrogen shift to vinylmethylene (INT3) followed by fragmentation to atomic hydrogen plus the propargyl radical (p1) and to $C_2H_2(X\,^1\Sigma_g^+) + CH_2(X\,^3B_1)$ (p2; 2%) (table 7). No elimination of molecular hydrogen was found experimentally or theoretically.

4.2.3. The $C(^3P_j)–H_2CCCH_2(X\,^1A_1)$ system

The crossed-molecular-beams technique supported by electronic structure and statistical calculations was also utilized to unravel the underlying dynamics of the reaction between ground-state carbon atoms $C(^3P_j)$ and the cummulene, allene (H_2CCCH_2) [331]. The reaction dynamics were found to be indirect via long lived intermediates. Dominated by large impact parameters, atomic carbon attacks the π system without entrance barrier at the terminal carbon atom of the allene molecule and forms a cyclopropylidene such as intermediate INT1 which is stabilized by $265 \, \text{kJ mol}^{-1}$ with respect to the reactants (figure 9). Trajectories with small impact parameters attack the central carbon atom of allene to yield INT2 which in turn isomerizes to INT1. Rather than undergoing a hydrogen shift via a large barrier of

Table 7. Reaction enthalpies of various exit channels of the reaction $C(^3P_j) + C_2H_4(X\,^1A_{1g})$. Enthalpies of formations of reactants and products are taken from [311].

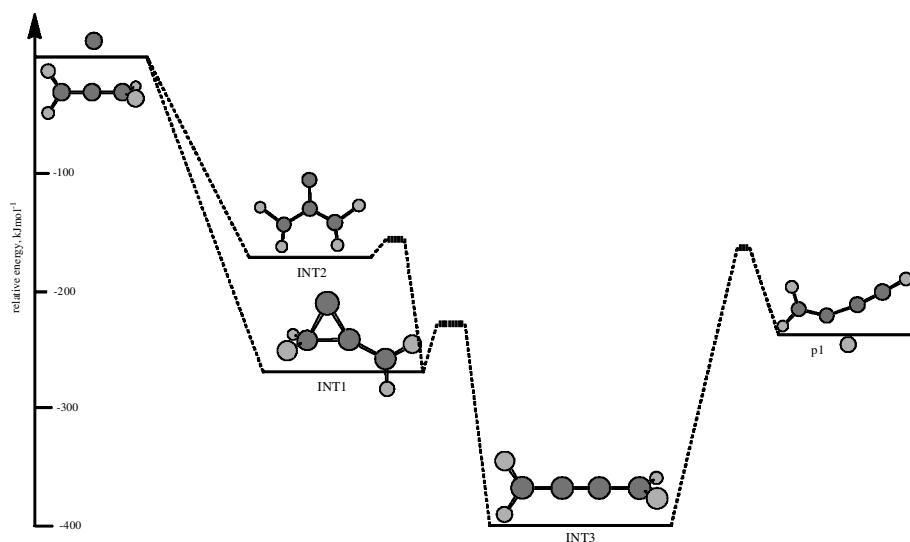| Products	Reaction enthalpy $(kJ\,mol^{-1})$
$C_3H_3(X\,^2B_1) + H(^2S_{1/2})$	-212.1
$C_3H_2(a\,^3A) + H_2(X\,^1\Sigma_g^+)$	-46.7
$HCCCH(X\,^3B) + H_2(X\,^1\Sigma_g^+)$	-213.1
$H_2CCC(a\,^3A'') + H_2(X\,^1\Sigma_g^+)$	-83.4
$CH_4(X\,^1A_1) + C_2(X\,^1\Sigma_g^+)$	-6.3
$CH_4(X\,^1A_1) + C_2(a\,^3\Pi_u)$	$+2.3$
$C_2H_3(X\,^2A') + CH(X\,^2\Pi_\Omega)$	$+124.0$
$2\,H_2(X\,^1\Sigma_g^+) + C_3(X\,^1\Sigma_g^+)$	$+50.9$
$CH_3(X\,^2A_2'') + C_2H(X\,^2\Sigma^+)$	-66.1
$C_2H_2(X\,^1\Sigma_g^+) + CH_2(X\,^3B_1)$	-156.1

Figure 9. Simplified PESs of the reaction of ground-state atomic carbon with allene. Carbon atoms are denoted in black, hydrogen atoms in grey.

about $200\,kJ\,mol^{-1}$, the INT1 ring opens through a barrier of only $39\,kJ\,mol^{-1}$ to a triplet butatriene species INT3. This molecule is bound by $405\,kJ\,mol^{-1}$ and decays via atomic hydrogen emission through an exit transition state lying $9\,kJ\,mol^{-1}$ above the products to the n-C_4H_3 isomer p1. Compared with the methylacetylene isomer and the reaction with ethylene, no carbon–carbon bond rupture was found to be important. The formation of $H_2CCC(X\,^1A_1) + CH_2(X\,^3B_1)$ from INT3 is endothermic and hence closed in cold molecular clouds (table 8).

Table 8. Reaction enthalpies of various exit channels of the reaction $C(^3P_j) + H_2CCCH_2(X\,^1A_1)$. Enthalpies of formations of reactants and products are taken from [311].

Products	Reaction enthalpy $(kJ\,mol^{-1})$
$n\text{-}C_4H_3(X\,^2A') + H(^2S_{1/2})$	-179.9
$C_4H_2(X\,^1\Sigma_g^+) + H_2(X\,^1\Sigma_g^+)$	-443.6
$C_4H_2(a\,^3\Pi_g) + H_2(X\,^1\Sigma_g^+)$	-58.1
$C_2H_4(X\,^1A_{1g}) + C_2(X\,^1\Sigma_g^+)$	-17.0
$C_2H_4(X\,^1A_{1g}) + C_2(a\,^3\Pi_u)$	-9.0
$C_3H_3(X\,^2B_1) + CH(X\,^2\Pi_\Omega)$	$+25.9$
$CH_4(X\,^1A_1) + C_3(X\,^1\Sigma_g^+)$	-162.0
$CH_4(X\,^1A_1) + C_3(a\,^3\Pi_u)$	$+40.5$
$C_2H_3(X\,^2A') + C_2H(X\,^2\Sigma^+)$	-52.1
$C_3H_2(X\,^1A_1) + CH_2(X\,^3B_1)$	-20.8
$HCCCH(X\,^3B) + CH_2(a\,^1A_1)$	$+35.2$
$H_2CCC(X\,^1A_1) + CH_2(X\,^3B_1)$	$+42.2$
$c\text{-}C_3H(X\,^2B_1) + CH_3(X\,^2A_2'')$	-38.4
$l\text{-}C_3H(X\,^2\Pi_\Omega) + CH_3(X\,^2A_2'')$	-31.3
$C_2H_2(X\,^1\Sigma_g^+) + C_2H_2(X\,^1\Sigma_g^+)$	-448.7
$C_2H_2(X\,^1\Sigma_g^+) + C_2H_2(a\,^3\Pi_u)$	-46.5

4.2.4. *The $C(^3P_j)$–$C_3H_5(X\,^2A_1)$ system*

The initial step of the reaction of atomic carbon $C(^3P_j)$ with the allyl radical $C_3H_5(X\,^2A_1)$ can lead to two different intermediates (figure 10) [332]. INT1 is produced by the atomic carbon addition to the terminal carbon atom of allyl without an entrance barrier and is stabilized by $299.7\,kJ\,mol^{-1}$ relative to the reactants. On the other hand, a bicyclic intermediate INT2, $399.6\,kJ\,mol^{-1}$ below $C(^3P_j) + C_3H_5(X\,^2A_1)$, is formed by the carbon addition between two terminal CH_2 groups of allyl, also without a barrier. INT1 is a metastable intermediate and can readily undergo a [1, 2]-H shift to the terminal carbenic carbon, forming the intermediate INT3. The INT1 $\rightarrow$ INT3 transition state exists at the B3LYP level of theory but at the higher G2M level its energy is $1.9\,kJ\,mol^{-1}$ lower than that of INT1, indicating that the hydrogen shift occurs (similar to the reactions of atomic carbon with two other hydrocarbon radicals vinyl and propargyl) virtually without a barrier. INT3 resides $516.9\,kJ\,mol^{-1}$ below the reactants. INT1 can also depict an insertion of the carbenic carbon into the neighbouring carbon–carbon bond, yielding intermediate INT4. The INT1 $\rightarrow$ INT4 barrier is only $8.4\,kJ\,mol^{-1}$, and INT4 is located $562.8\,kJ\,mol^{-1}$ lower in energy than $C(^3P_j) + C_3H_5(X\,^2A_1)$. One can imagine another pathway leading from the reactants to INT4, the atomic carbon addition to the carbon–carbon bond of allyl, forming a cyclic intermediate followed by the three-membered ring opening, similar to the reaction of carbon atoms with olefines. However, the calculations have shown that the $(CH_2CCH)CH_2$ cyclic structure is not a local minimum on the PES. Since INT1 is a metastable species, one cannot exclude that some descending trajectories exist on the surface leading from the reactants to INT4, where the atomic carbon approaches a terminal carbon atom of allyl or the carbon–carbon bond. The third channel of isomerization of INT1 involves rotation
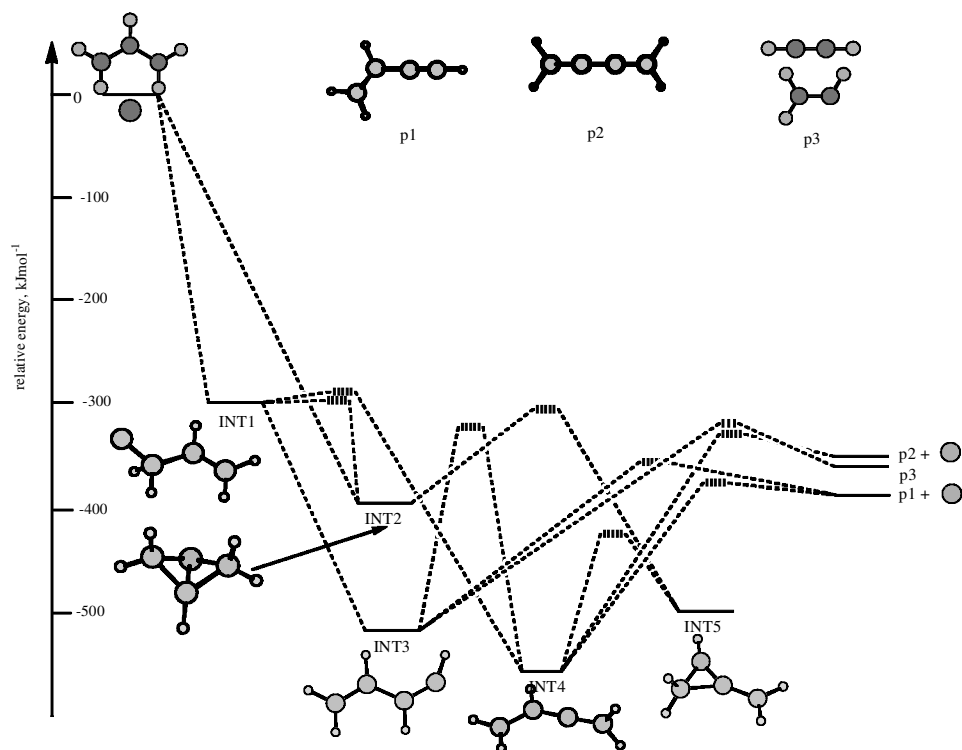
Figure 10. Simplified PESs of the reaction of ground-state atomic carbon with the allyl radical. Carbon atoms are denoted in black, and hydrogen atoms in grey.

around the C–CH$_2$C bond, resulting in the bicyclic structure INT2. The calculated barrier is 5.8 kJ mol^{-1} and the INT1 → INT2 rearrangement is about 100 kJ mol^{-1} exothermic. Opening of one of the rings in INT2 yields another cyclic intermediate INT5 via a barrier of 98.5 kJ mol^{-1}. INT5 is positioned 494.3 kJ mol^{-1} below the reactants and can undergo the second ring opening, leading to INT4 with a barrier of 70.4 kJ mol^{-1}.

We investigate now possible fragmentation pathways of the intermediates involved. INT3 and INT4 can lose a hydrogen atom, producing the vinylacetylene (p1), the most stable isomer of the singlet C$_4$H$_4$ PES, and butatriene (p2). The exothermicities of the C(^{3}P$_j$) + C$_3$H$_5$(X^{2}A$_1$) C$_4$H$_4$(X^{1}A') (p1) + H(^{2}S$_{1/2}$) and C(^{3}P$_j$) + C$_3$H$_5$(X^{2}A$_1$) C$_4$H$_4$(X^{1}A$_g$) (p2) + H(^{2}S$_{1/2}$) reactions are calculated as 382.8 and 351.6 kJ mol^{-1}, respectively (table 9). p1 is produced by a hydrogen atom elimination from INT3 and INT4 with the exit barriers of 24.6 and 8.1 kJ mol^{-1}, while p2 can be formed solely from INT4 via an exit barrier of 20.2 kJ mol^{-1}. Additionally, a carbon–carbon bond cleavage in INT3 yields vinyl plus acetylene (p3) with an exit barrier of 24.7 kJ mol^{-1} and the total reaction exothermicity of 360 kJ mol^{-1}. Preliminary RRKM calculations show that the p1 versus the p3 branching ratio is very sensitive to the relative concentrations of INT1 and INT2 formed after the initial collision. Assuming that only INT1 is produced, the calculated p1 and p3 branching ratios are 29.5% and 70.1% respectively, and for the opposite limiting case (100% of INT2) the p1 and p3 branching ratios change to

Table 9. Reaction enthalpies of various exit channels of the reaction $C(^3P_j) + C_3H_5(X\,^2A_1)$. Enthalpies of formations of reactants and products are taken from [311].

Products	Reaction enthalpy $(kJ\,mol^{-1})$
$HCCC_2H_3(X\,^1A') + H(^2S_{1/2})$	-382.6
$C_4H_3(X\,^2A') + H_2(X\,^1\Sigma_g^+)$	-378.4
$C_2H_5\,(X\,^2A') + C_2(X\,^1\Sigma_g^+)$	$+69.1$
$CH_3CCH(X\,^1A_1) + CH(X\,^2\Pi_\Omega)$	-108.2
$H_2CCCH_2(X\,^1A_1) + CH(X\,^2\Pi_\Omega)$	-103.1
$C_2H_4(X\,^1A_{1g}) + C_2H(X\,^2\Sigma^+)$	-105.0
$C_3H_3(X\,^2B_1) + CH_2(X\,^3B_1)$	-162.3
$CH_4(X\,^1A_1) + c\text{-}C_3H(X\,^2B_1)$	-245.8
$CH_4(X\,^1A_1) + l\text{-}C_3H(X\,^2\Pi_\Omega)$	-238.7
$C_2H_3(X\,^2A') + C_2H_2(X\,^1\Sigma_g^+)$	-362.0
$c\text{-}C_3H_2(X\,^1A_1) + CH_3(X\,^2A_2'')$	-240.7
$HCCCH(X\,^3B) + CH_3(X\,^2A_2'')$	-184.7
$H_2CCC(X\,^1A_1) + CH_3(X\,^2A_2'')$	-177.7

62.1% and 36.2% respectively. Butatriene (p2) gives only a minor contribution, 0.4–1.7%. These results indicate that the branching ratio of vinylacetylene plus hydrogen and of vinyl plus acetylene should strongly depend on the collision impact parameter. For instance, small impact parameters should favour the formation of INT2 and increase the contribution of vinylacetylene. Meanwhile, other product channels may also be possible, including a possible H_2 loss leading to n- and i-C_4H_3 (exothermic by 378.4 and 332.8 kJ mol^{-1} respectively (table 9)), a carbon–carbon bond cleavage in INT4 yielding propargyl plus carbene and allene plus methylidene (from INT5), or a hydrogen migration in INT4 followed by a methyl group elimination. The formation of CH_4 is less likely because it requires a large number of hydrogen migrations in the C_4H_5 intermediates; similar arguments suggest that a methyl group elimination is also closed. A *b-initio* and RRKM calculations of the complete PES are now under way.

4.2.5. *The $C(^3P_j)$–$C_3H_6(X\,^1A')$ system*

The reaction of propylene with atomic carbon proceeds on the triplet surface via indirect scattering dynamics and is initiated by a barrierless addition of atomic carbon to the π bond [333, 334]. This forms a three-membered methylcyclopropylidene intermediate (INT1) which resides in a potential energy well of 218 kJ mol^{-1} (figure 11). Rather than undergoing hydrogen migration to methylcyclopropene, the INT1 ring opens to a triplet methylallene intermediate (INT2). This exists in a *trans* and a *cis* form, which are 242 kJ mol^{-1} and 244 kJ mol^{-1} more stable than their precursor. Similar to the ethylene system, these structures fragment predominantly via tight exit transition states located 18–23 kJ mol^{-1} above the separated products by atomic hydrogen loss. The experimental data support the existence of exit barriers as the centre-of-mass translation energy distributions peak at 28–60 kJ mol^{-1}. This leads to three C_4H_5 isomers 1,3-butadienyl-2 (H_2CHCCH_2(p3; $X\,^2A'$)), 1-methylpropargyl ((CH_3)HCCCH(p1; $X\,^2A''$)), and 3-methylpropargyl ((CH_3)CCCH$_2$(p2;
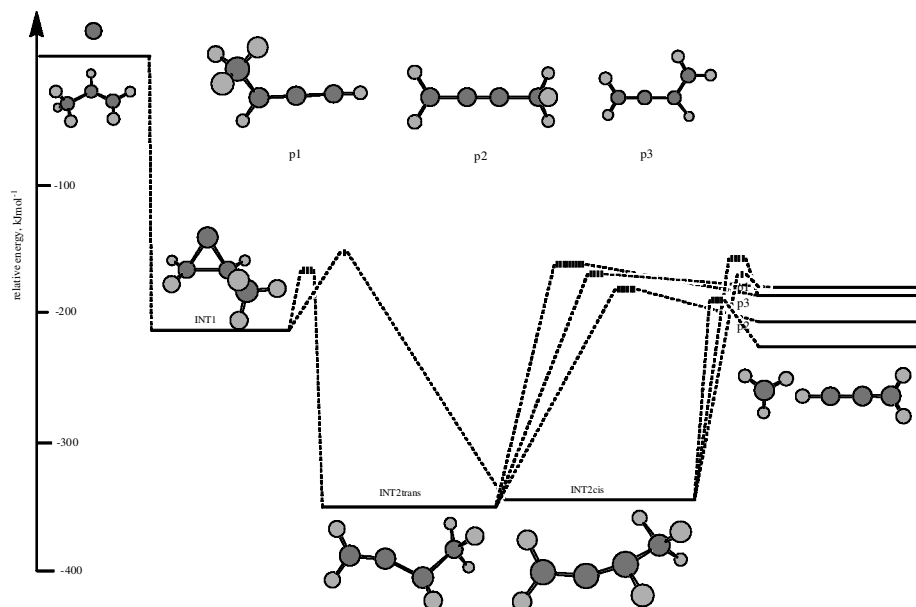
Figure 11. Simplified PESs of the reaction of ground-state atomic carbon with propylene. Carbon atoms are denoted in black, and hydrogen atoms in grey.

X^2A'')) in a ratio of about 3.7:2.8:1 (C_3H_6 system) in strongly exoergic reactions (190–210 kJ mol^{-1}). This hydrogen loss was also confirmed experimentally. However, compared with the $C(^3P_j)$–$C_2H_4(X^1A_{1g})$ system, no direct microchannel could be identified experimentally. The electronic calculations predict that INT2 should also decompose via homolytic cleavage of a carbon–carbon single bond to form $C_3H_3(X^2B_1)$ + $CH_3(X^2A_2'')$ to about 16% (table 10). Note that the latter pathway is

Table 10. Reaction enthalpies of various exit channels of the reaction $C(^3P_j)$ + $C_3H_6(X^1A')$. Enthalpies of formations of reactants and products are taken from [311].

Products	Reaction enthalpy (kJ mol^{-1})
$CH_3CCCH_2(X^2A'')$ + $H(^2S_{1/2})$	-200.8
$HCCC_2H_3(X^1A')$ + $H_2(X^1\Sigma_g^+)$	-442.1
$C_3H_5(X^2B_1)$ + $CH(X^2\Pi_\Omega)$	$+28.1$
$C_2H_6(X^1A_{1g})$ + $C_2(X^1\Sigma_g^+)$	$+16.9$
$C_2H_5 (X^2A')$ + $C_2H(X^2\Sigma^+)$	$+62.1$
$CH_3CCH(X^1A_1)$ + $CH_2(X^3B_1)$	-165.3
$H_2CCCH_2(X^1A_1)$ + $CH_2(X^3B_1)$	-160.2
$C_2H_4(X^1A_{1g})$ + $C_2H_2(X^1\Sigma_g^+)$	-457.9
$C_3H_3(X^2B_1)$ + $CH_3(X^2A_2'')$	-251.1
$C_3H_2(X^1A_1)$ + $CH_4(X^1A_1)$	-312.0
$HCCCH(X^3B)$ + $CH_4(X^1A_1)$	-256.0
$H_2CCC(X^1A_1)$ + $CH_4(X^1A_1)$	-249.0
$C_2H_3(X^2A')$ + $C_2H_3(X^2A')$	-139.1

unobservable employing 'universal' detectors owing to the significant background at the masses of interest from the parent molecules. Once again, a molecular hydrogen elimination is absent, and the endoergic channels $C_3H_5(X\,^2B_1) + CH(X\,^2\Pi_\Omega)$, $C_2H_6(X\,^1A_{1g}) + C_2(X\,^1\Sigma_g^+)$, and $C_2H_5(X\,^2A') + C_2H(X\,^2\Sigma^+)$ cannot be opened in molecular clouds. Although the remaining pathways are exoergic, they do not contribute to the reaction dynamics of the $C(^3P_j)$–$C_3H_6(X\,^1A')$ system. Considering the intermediates involved, neither INT1 nor INT2 connects to the $C_3H_4 + CH_2(X\,^3B_1)$, $C_3H_2 + CH_4(X\,^1A_1)$, and $C_2H_3(X\,^2A') + C_2H_3(X\,^2A')$ reaction products. Likewise, the spin-forbidden $C_2H_4(X\,^1A_{1g}) + C_2H_2(X\,^1\Sigma_g^+)$ pathway is also closed. A hypothetical carbon–carbon bond rupture in INT2 would lead to the singlet vinylidene (H_2CC) + triplet methylcarbene ($HCCH_3$) isomers, but the reaction is endoergic by 43.8 kJ mol^{-1} [335]. Therefore, we conclude that the atomic hydrogen and methyl group elimination pathways are the only feasible channels in the reaction of carbon atoms with propene.

4.2.6. *The $C(^3P_j)$–C_2H_3-$C_2H_3(X\,^1A')$ system*

The reaction of atomic carbon with 1,3-butadiene proceeds without entrance barrier on the triplet surface via indirect scattering dynamics and is initiated by an addition of $C(^3P_j)$ to the carbon–carbon double bond. This process yields a vinyl substituted cyclopropenylidene intermediate INT1 in its *trans* form (figure 12) [336]. This structure is stabilized by 213 kJ mol^{-1} with respect to the reactants and is ring open via a barrier of only 51.5 kJ mol^{-1} to vinylallene (INT2). Competing hydrogen shifts to (substituted) cyclopropene intermediates are unfavourable as these processes involve significant barriers of 200–210 kJ mol^{-1}. The allene derivative is located in a deep potential energy well of 359.8 kJ mol^{-1}. As verified experimentally by isotopically labeled 1,3-butadiene, the predominant exit channels are two
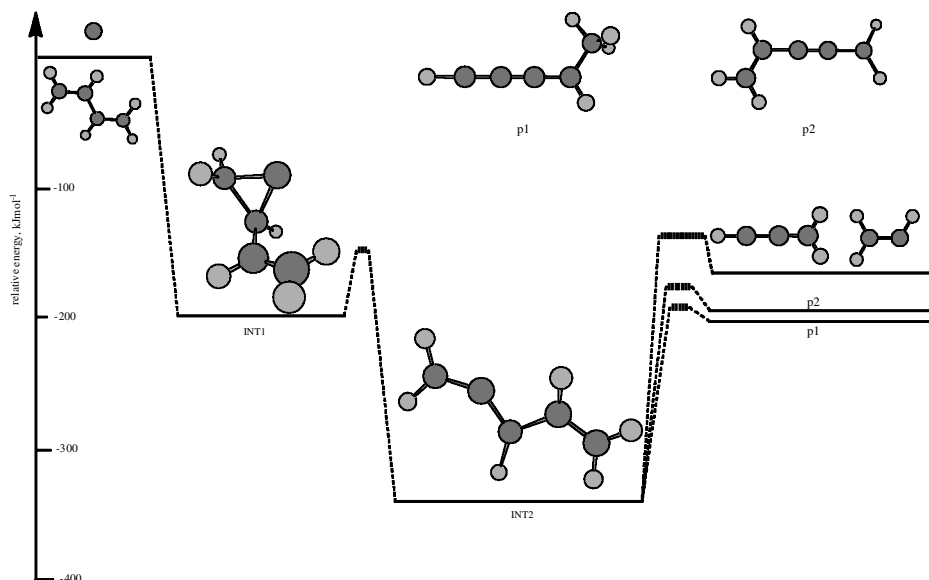

Figure 12. Simplified PESs of the reaction of ground-state atomic carbon with 1,3-butadiene. Carbon atoms are denoted in black, and hydrogen atoms in grey.

hydrogen loss pathways via tight transition states to give 1-vinylpropargyl (HCCCH(C_2H_3)(p1; $X\,^2A''$) and 3-vinylpropargyl $H_2CCC(C_2H_3)$(p2; $X\,^2A''$) isomers in a ratio of 8:1 in exoergic reactions ($-209.6\,kJ\,mol^{-1}$ and $196.2\,kJ\,mol^{-1}$ respectively). Additional RRKM calculations show that, in strong analogy to the triplet methylallene intermediate in the $C(^3P_j)$–C_3H_6($X\,^1A'$) system, INT2 can also lose the vinyl substituent to form C_2H_3($X\,^2A'$) + C_3H_3($X\,^2B_1$) to less than 10%. Although various other pathways are open energetically (table 11), neither INT1 nor INT2 connects to these products. Note that homolytic bond cleavages of the propargyl moiety could lead to triplet carbene (CH_2) plus singlet vinyl-substituted vinylidene ($CC(C_2H_3)H$) and singlet vinylidene (H_2CC) plus triplet vinylcarbene ($HC(C_2H_3)$). These exit channels hold reaction enthalpies of $-1.3\,kJ\,mol^{-1}$ [337] and $+16.6\,kJ\,mol^{-1}$ and, hence, are strongly expected to be unimportant.

4.2.7. *The $C(^3P_j)$–$H_2CCCH(CH_3)$($X\,^1A'$) system*

The *ab-initio* calculations and crossed-beams data reveal that the reaction is initiated by a barrierless addition of the carbon atom to the π system of the 1,2-butadiene molecule [264, 338]. Dominated by large impact parameters, $C(^3P_j)$ attacks preferentially the C(2)–C(3) double bond, yielding INT1 (mechanism 1); to a minor amount, small impact parameters lead to an addition of atomic carbon to the C(1)–C(2) bond forming INT2 (mechanism 2) (figure 13). Both cyclic inter-

Table 11. Reaction enthalpies of various exit channels of the reaction $C(^3P_j)$ + C_2H_3–C_2H_3($X\,^1A'$). Enthalpies of formations of reactants and products are taken from [311].

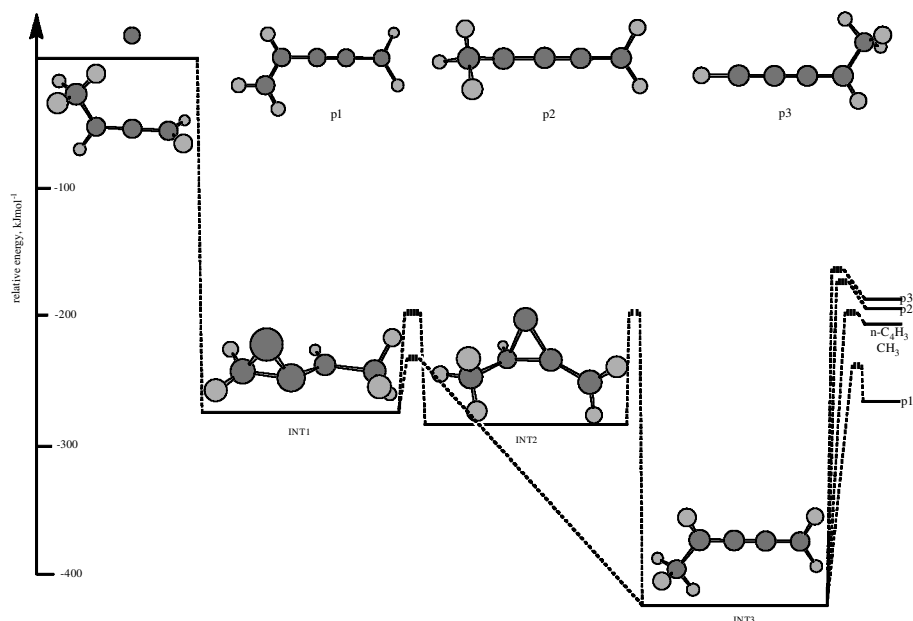| Products	Reaction enthalpy ($kJ\,mol^{-1}$)
HCCCH(C_2H_3)($X\,^2A''$) + H($^2S_{1/2}$)	-209.6
$H_2CCCCCH_2$($X\,^1A_g$) + H_2($X\,^1\Sigma_g^+$)	-360.0
C_2($X\,^1\Sigma_g^+$) + C_3H_6($X\,^1A'$)	$+32.9$
C_2($a\,^3\Pi_u$) + C_3H_6($X\,^1A'$)	$+40.9$
CH($X\,^2\Pi_\Omega$) + CH_3CCCH_2($X\,^2A''$)	$+87.2$
C_3($X\,^1\Sigma_g^+$) + C_2H_6($X\,^1A_{1g}$)	-88.4
C_3($a\,^3\Pi_u$) + C_2H_6($X\,^1A_{1g}$)	$+111.6$
C_2H($X\,^2\Sigma^+$) + C_3H_5($X\,^2B_1$)	-177.2
CH_2($X\,^3B_1$) + $HCCC_2H_3$($X\,^1A'$)	-143.8
c-C_3H($X\,^2B_1$) + C_2H_5 ($X\,^2A'$)	-10.5
l-C_3H($X\,^2\Pi_\Omega$) + C_2H_5($X\,^2A'$)	$+17.6$
C_2H_2($X\,^1\Sigma_g^+$) + CH_3CCH($X\,^1A_1$)	-413.1
C_2H_2($a\,^3\Pi_u$) + CH_3CCH($X\,^1A_1$)	-10.9
C_2H_2($X\,^1\Sigma_g^+$) + H_2CCCH_2($X\,^1A_1$)	-408.0
C_2H_2($a\,^3\Pi_u$) + H_2CCCH_2($X\,^1A_1$)	-5.6
CH_3($X\,^2A_2''$) + n-C_4H_3($X\,^2A'$)	-170.2
c-C_3H_2($X\,^1A_1$) + C_2H_4($X\,^1A_{1g}$)	-272.7
HCCCH($X\,^3B$) + C_2H_4($X\,^1A_{1g}$)	-216.7
H_2CCC($X\,^1A_1$) + C_2H_4($X\,^1A_{1g}$)	-209.3
C_2H_3($X\,^2A'$) + C_3H_3($X\,^2B_1$)	-187.2
CH_4($X\,^1A_1$) + C_4H_2($X\,^1\Sigma_g^+$)	-436.1
CH_4($X\,^1A_1$) + C_4H_2($a\,^3\Pi_g$)	-50.6

Figure 13. Simplified PESs of the reaction of ground-state atomic carbon with 1,2-
butadiene. Carbon atoms are denoted in black, and hydrogen atoms in grey.

mediates are stabilized by 275.9 kJ mol^{-1} and 280.9 kJ mol^{-1} respectively and is ring open to triplet methylbutatriene intermediates INT3. The equilibrium structure is bound by 430.4 kJ mol^{-1} with respect to the reactants. Similar to the reaction of atomic carbon with ethynyl, propargyl and vinyl, two distinct intermediates arise. Denoting the incorporated carbon atom in bold, these are INT3$'$ (H$_2$C**C**CCH(CH$_3$)) and INT3$''$ (H$_2$CCC**C**H(CH$_3$)). INT3$'$ is suggested to decay non-statistically prior to a complete energy randomization via atomic hydrogen loss forming 1- and 4-methylbutatrienyl CH$_3$CCCCH$_2$(X ^{2}A$''$) and HCCCCH(CH$_3$)(X ^{2}A$''$) respectively; at higher collision energies, this pathway was found to be direct. The energy randomization in INT3$''$ is likely to be complete. The reaction dynamics are indirect, and INT3$''$ decomposes via hydrogen atom loss to 3-vinylpropargyl, H$_2$CCCCC$_2$H$_3$(X ^{2}A$''$), as well as 1- and 4-methylbutatrienyl radicals. RRKM calculations suggest further that CH$_3$(X ^{2}A$_2''$) + n-C$_4$H$_3$(X ^{2}A$'$) (table 12) contributes about 10%. Analogous to the reaction of atomic carbon with both 1,3-butadiene and dimethylacetylene, no molecular hydrogen elimination was observed experimentally. Likewise, the propargyl moiety is conserved, and no bond rupture at the C(1)–C(3) atoms is feasible energetically.

4.3. *Reactions of atomic carbon with aromatic hydrocarbons*

The dynamics of the reaction of atomic carbon with benzene C$_6$H$_6$(X ^{1}A$_{1g}$) were investigated at collision energies between 8.8 and 52.5 kJ mol^{-1} [339–341]. Supported by electronic structure calculations, these studies showed that similar to the reactions with olefines and allenes the carbon atom adds in a barrierless way to the π system, yielding a weakly stabilized INT1 intermediate on the triplet surface (−62 kJ mol^{-1} (figure 14)). The latter isomerizes to a seven-membered ring inter-

Table 12. Reaction enthalpies of various exit channels of the reaction $C(^3P_j)$ + $H_2CCCH(CH_3)(X^1A')$. Enthalpies of formations of reactants and products are taken from [311].

Products	Reaction enthalpy $(kJ\,mol^{-1})$
$H_2CCC(C_2H_3)(X^2A'') + H(^2S_{1/2})$	-259.8
$H_2CCCCCH_2(X^1A_g) + H_2(X^1\Sigma_g^+)$	-413.5
$C_2(X^1\Sigma_g^+) + C_3H_6(X^1A')$	-20.8
$C_2(a^3\Pi_u) + C_3H_6(X^1A')$	-12.8
$CH(X^2\Pi_\Omega) + CH_3CCCH_2(X^2A'')$	$+33.5$
$C_3(X^1\Sigma_g^+) + C_2H_6(X^1A_{1g})$	-142.1
$C_3(a^3\Pi_u) + C_2H_6(X^1A_{1g})$	$+57.9$
$C_2H(X^2\Sigma^+) + C_3H_5(X^2B_1)$	-230.9
$CH_2(X^3B_1) + HCCC_2H_3(X^1A')$	-197.5
$c\text{-}C_3H(X^2B_1) + C_2H_5\ (X^2A')$	-43.2
$l\text{-}C_3H(X^2\Pi_\Omega) + C_2H_5(X^2A')$	-36.1
$C_2H_2(X^1\Sigma_g^+) + CH_3CCH(X^1A_1)$	-466.8
$C_2H_2(a^3\Pi_u) + CH_3CCH(X^1A_1)$	-64.6
$C_2H_2(X^1\Sigma_g^+) + H_2CCCH_2(X^1A_1)$	-461.7
$C_2H_2(a^3\Pi_u) + H_2CCCH_2(X^1A_1)$	-59.3
$CH_3(X^2A_2'') + n\text{-}C_4H_3(X^2A')$	-223.9
$c\text{-}C_3H_2(X^1A_1) + C_2H_4(X^1A_{1g})$	-326.4
$HCCCH(X^3B) + C_2H_4(X^1A_{1g})$	-270.4
$H_2CCC(X^1A_1) + C_2H_4(X^1A_{1g})$	-263.4
$C_2H_3(X^2A') + C_3H_3(X^2B_1)$	-240.9
$CH_4(X^1A_1) + C_4H_2(X^1\Sigma_g^+)$	-489.8
$CH_4(X^1A_1) + C_4H_2(a^3\Pi_g)$	-104.3

mediate INT2 ($-294\,kJ\,mol^{-1}$) followed by a barrierless hydrogen atom elimination to a 1,2-didehydrocycloheptatrienyl radical $C_7H_5(X^2B_1)$. The overall reaction enthalpy was found to be $-15.6 \pm 4.8\,kJ\,mol^{-1}$. The reaction dynamics change significantly with the collision energy. At low collision energies the dynamics are indirect and dominated by large impact parameters. With increasing collision energy, smaller impact parameters become increasingly significant, and the chemical dynamics are more direct. In case of reactions with per-deuterobenzene, the formation of a C_7D_6 adduct which has a lifetime of a few hundred microseconds at lower collision energies is also observed.

5. Summary
5.1. Reaction of atomic carbon with hydrocarbons carrying carbon–carbon triple bonds

Our combined experimental and theoretical studies presented generalized concepts on the reactivities of ground state carbon atoms $C(^3P_j)$ with alkynes and alkynyl radicals. All reactions have no entrance barrier and proceed via an addition of atomic carbon atom to the carbon–carbon triple bond. No evidence of an insertion of the carbon atom into a carbon–hydrogen σ bond was found. Upon reaction with closed-shell alkynes, the initial addition pathways of $C(^3P_j)$ form either substituted propenediylidene or cyclopropenylidene intermediates which are stabi-
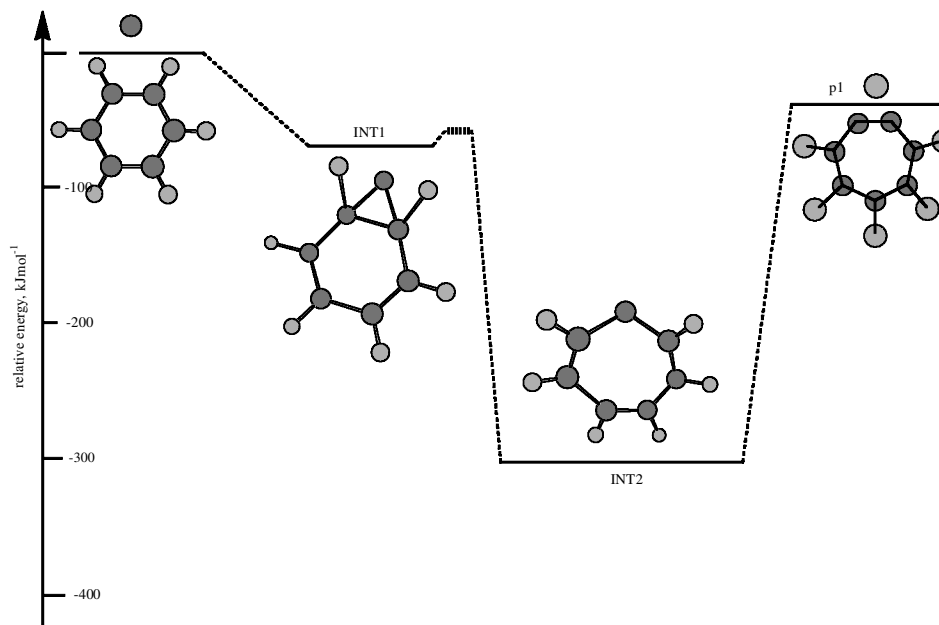
Figure 14. Simplified PESs of the reaction of ground-state atomic carbon with benzene. Carbon atoms are denoted in black, and hydrogen atoms in grey.

lized by 122–137 kJ mol^{-1} and 190–225 kJ mol^{-1} respectively. The propenediylidenes exist in either a *trans* or a *cis* form which are separated by low barriers of only 8–10 kJ mol^{-1}. The *cis* forms undergo ring closure to cyclopropenylidenes through barriers of 1–18 kJ mol^{-1} and facile hydrogen shift to (substituted) propargylene derivatives via barriers of 0.1–11 kJ mol^{-1}. These propargylene intermediates are bound by typically 352–388 kJ mol^{-1} with respect to the reactants and can be formed also via ring opening from cyclopropenylidenes; the barriers involved are about 55–65 kJ mol^{-1} above the corresponding propenediylidene structures. All propargylene structures fragment mainly via atomic hydrogen elimination in a barrierless way (C_2H_2 reaction) or through tight exit transition states located 19–24 kJ mol^{-1} above the products. In all the systems studied, chain isomers are predominantly formed; cyclic reaction products are only found in the $C-C_2H_2$ reaction ($c-C_3H$) and possibly also in the $C-C_2H$ ($c-C_3$) and $C-CH_3CCH$ ($c-C_4H_3$) systems. The $C(^3P_j) + C_2H_2$ reaction is of particular importance as ISC from the triplet to the singlet manifold is facile; here, elimination of molecular hydrogen is also an important pathway. To a minor amount of a few per cent at most, the intermediates can decompose also via homolytic cleavages of carbon–carbon bonds to form low-mass hydrocarbon fragments $C_4H + H_2$ and $C_2H_2 + C_2H$ ($C-C_3H_3$ system) together with $C_3H + CH_3$ ($C-CH_3CCH$ system).

5.2. *Reaction of atomic carbon with hydrocarbons carrying carbon–carbon double bonds*

The crossed-beams investigations and electronic structure calculations on the reactions of carbon atoms with olefines, cummulenes and also benzene showed explicitly that all reactions have no entrance barrier. They are further initiated by an

addition of the carbon atom to the π bond; an insertion into carbon–carbon or carbon–hydrogen σ bonds does not take place. With the exception of the atom radical reactions C–C_2H_3 and C–C_3H_5, which shows also initial chain intermediates, the addition pathway leads solely to three-membered cyclopropylidene intermediates which are stabilized by about 213–217 kJ mol^{-1} (closed-shell olefines) and 265–281 kJ mol^{-1} (cummulenes) compared with the reactants. The latter are ring open to (substituted) propargyl structures and reside in deep potential energy wells of 342–360 kJ mol^{-1} (closed-shell olefines) and 405–430 kJ mol^{-1} (cummulenes). Isomerization from cyclopropylidene intermediates via hydrogen shifts to form triplet (substituted) cyclopropene structures are insignificant because the inherent barriers are about 200 kJ mol^{-1} compared with barriers for the ring-opening processes of only 58 kJ mol^{-1} at most. This is in strong contrast with the alkyne systems studied, as hydrogen migrations were found to be important as well. The intermediates involved fragment predominantly via atomic hydrogen elimination to yield chain-like isomers through tight exit transition states (closed-shell reactants); to a minor amount, the C–C_2H_3 system forms also cyclic structures (c-C_3H_2); the reaction of atomic carbon with benzene gives solely a cyclic reaction products. No evidence for an ISC was found. In contrast with the alkyne systems, carbon–carbon bond ruptures are more important (10–16%); in all cases except the ethylene and vinyl reactions, in which the C_2H_2 + CH_2 (less than 2%) and CH + C_2H_2 (less than 0.4%) pathways are open as well, the propargyl moieties are conserved; the methyl and vinyl groups are released.

5.3. *Statistical and non-statistical decomposition of the reaction intermediates*

Our investigations provided evidence that the chemical dynamics of reactions of atomic carbon with unsaturated hydrocarbons strongly depend on particular reactive impact parameters. The impact-parameter-dependent formation of distinct intermediates possibly holds the key for the non-statistical behaviour found experimentally in carbon atom reactions with acetylene, 1,2-butadiene and probably also with methylacetylene and the propargyl radical. It is important to stress that the RRKM treatment superimpose a complete energy randomization in the decomposing intermediate upon formation of the new bond; this intramolecular energy distribution is postulated to be rapid before the final carbon–hydrogen bond ruptures takes place. Therefore, any RRKM-based investigation cannot discriminate between discrete intermediates of the same isomer formed via distinct microchannels. Figure 15 shows those decomposing intermediates, which reflect impact-parameter-dependent formation routes. In each intermediate shown, the arrows originating from the incorporated carbon atoms point to different carbon–hydrogen bonds which can be cleaved homolytically; data in italics define the number of connectivities over which the energy has to 'flow' from the chemically activated bond to the carbon–hydrogen link to be cut.

The reaction of C(^3P_j) with 1,2-butadiene serves as a typical example to rationalize common trends (figure 15 (*g*)). The reactant carbon atom can be located at the C(2) or C(3) position of the triplet methylbutatriene intermediate (section 4.2.7). Large impact parameters dominated the reaction and locate the reacting carbon atom predominantly at C(2), whereas, to a minor extent, smaller impact parameters trigger the location at C(3). The formation of the energetically most favourable 4-vinylpropargyl radical (figure 14, p4) requires the energy to be transferred over four (C(2)) and three (C(3)) bonds from the 'initially activated bond' to
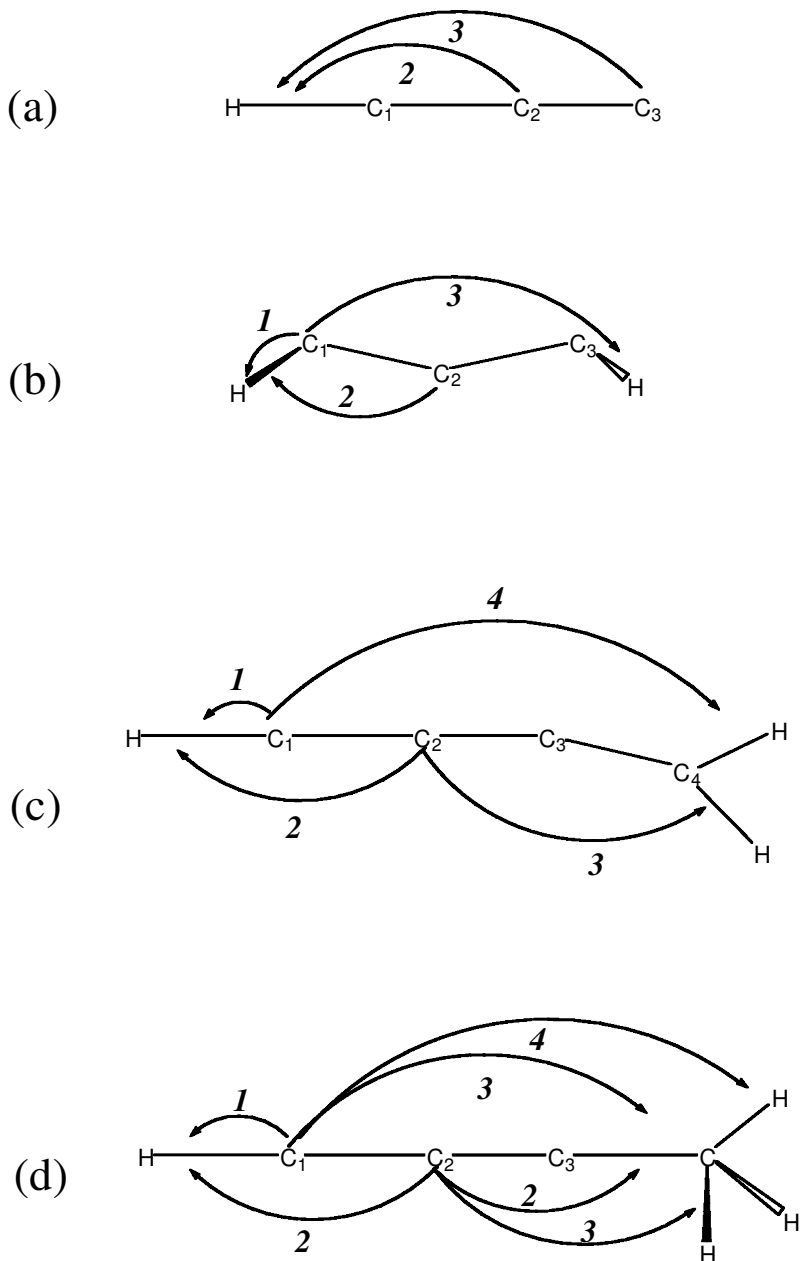
Figure 15

the carbon–hydrogen bond of the methyl group. Since p4 was found to be only a minor product of the reaction, the energy randomization in the intermediate in which the carbon atom is located at C(2) is probably not completed. Otherwise, if the energy was statistically distributed before the bond broke, a prevailing formation of p4 should have been observed experimentally. Here, an energy 'flow' only over fewer than four bonds leads to the emission of a hydrogen atom.
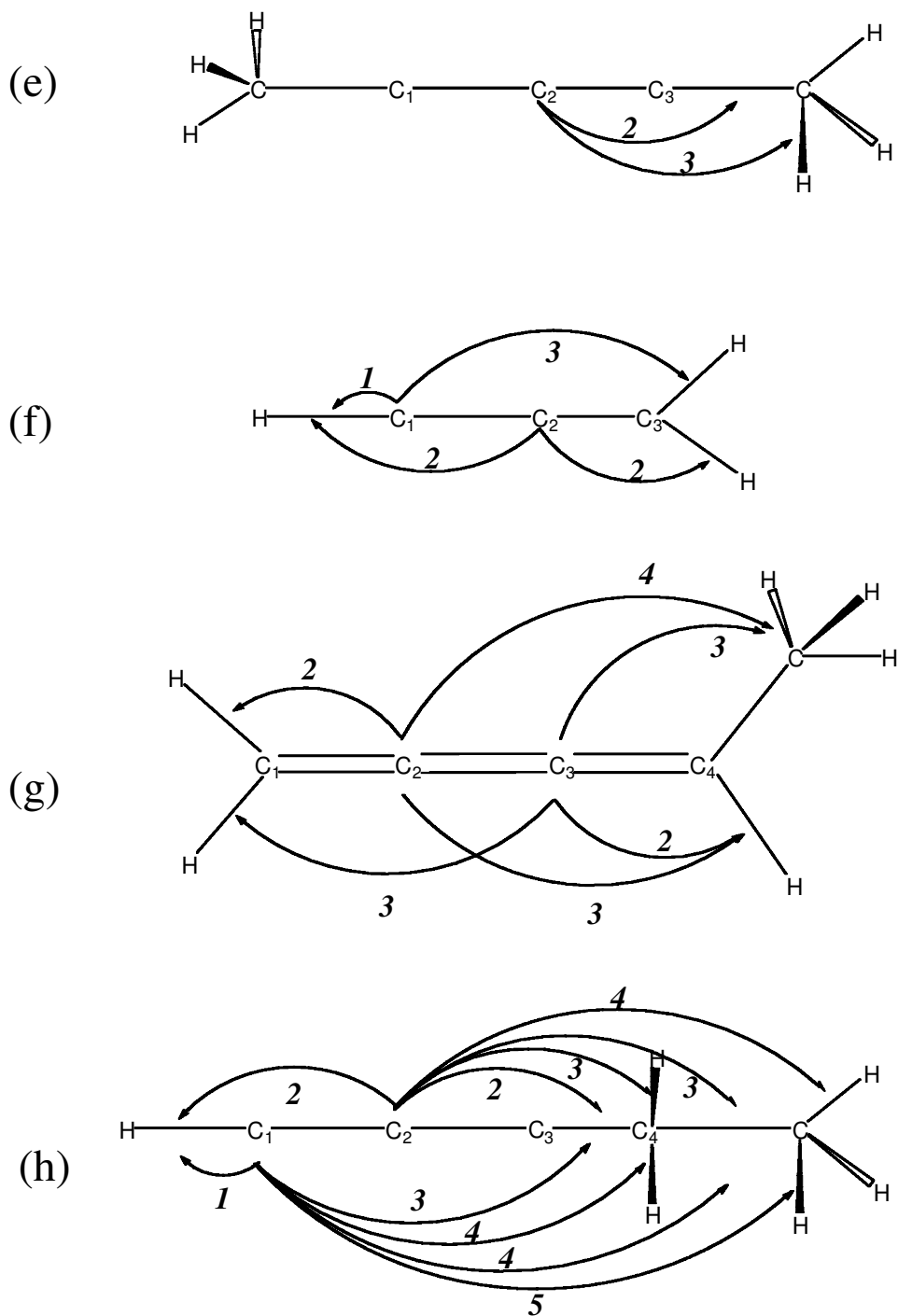
Figure 15. Various carbon–hydrogen bond cleavages in distinct decomposing intermediates involved in the reaction of atomic carbon with (*a*) ethynyl, (*b*) acetylene, (*c*) propargyl, (*d*) methylacetylene, (*e*) dimethylacetylene, (*f*) vinyl, (*g*) 1,2-butadiene, and (*h*) ethylacetylene. Data given in italics indicate the number of bonds from the incorporated carbon atom to the hydrogen atom to be released.

This concept can be utilized to explain the statistical and non-statistical patterns in the reactions of carbon with methylacetylene (section 4.1.4), dimethylacetylene (section 4.1.5) and the propargyl radical (section 4.1.3). The C–CH_3CCH reaction proceeds via a triplet methylpropargylene intermediate (figure 15 (*d*)) in which the reacting carbon atom can be found at the C(1) (formed with large impact parameters) or C(2) position (smaller impact parameters). The C(2) intermediates fragmented to the n-C_4H_3 isomer; this process involves the energy to 'channel' over three bonds. However at lower collision energies, it is suggested that the C(1) intermediates do not necessarily have to react via ejection of a hydrogen atom (an energy over four bounds would be involved in this process), but might undergo isomerization via ring closure prior to a hydrogen atom emission to form a cyclic C_4H_3 reaction product. In the related C–CH_3CCCH_3 system, the carbon atom was found only in the central C(2) position (figure 15 (*e*)); this intermediate fragments via carbon–hydrogen bond rupture to form the CH_3CCCCH_2 isomer—a process which consist of an energy transfer over two bonds. The situation in the reaction of atomic carbon with the propargyl radical is similar to the methylacetylene reactant. Again, the carbon atom can be placed at C(1) or C(2) (figure 15 (*c*)). The C(2) isomer was found to decompose to diacetylene plus atomic hydrogen (energy flow via three bonds); this was strongly supported by the centre-of-mass angular distribution depicting that the incorporated carbon atom (here C(2)) and the released hydrogen atom must be located at opposite sites of the rotational axis. A carbon atom placed at C(1) cannot account for this requirement. So far, the fate of these intermediates in unknown; a possible fragmentation to the thermodynamically less stable $CCCCH_2$ isomer might present one option.

These patterns help us to unravel also the chemical dynamics of the reaction of atomic carbon with ethylacetylene (C_2H_5CCH). The latter presents, besides di-methylacetylene, 1,3-butadiene and 1,2-butadiene, a fourth closed-shell and stable C_4H_6 isomer. Crossed-beams experiments were also performed with this molecule; however, no reactive scattering signal of an atomic or molecular hydrogen loss channel was observed [342]; accounting for the signal-to-noise ratio, the carbon versus hydrogen exchange pathway was found to be less than 5% involved compared with the C–CH_3CCH system. At the first glance, this finding is highly unusual as the reaction should proceed via addition to the carbon–carbon triple followed by isomerizations to the triplet ethylpropargylene intermediate (figure 15 (*h*)). Since the reaction has no entrance barrier, a large impact parameter should dominate, and the carbon atom should be located preferentially at C(1); smaller impact parameters direct it towards the C(2) position. The bulky ethyl group is also expected to reduce the cone of acceptance of the adjacent carbon atom significantly, thus supporting the formation of C(1) intermediates. A cleavage of the H−C(1) bond forming the $CCCC_2H_5$ isomer is energetically unfavourable, and the overall reaction is calculated to be $15.7\,kJ\,mol^{-1}$ exoergic. The emission of atomic hydrogen from the C(4)–H bond would yield the 4-methylbutatrienyl radical in a strongly exoergic reaction. However, this mechanism requires the energy to 'flow' over four bonds from the chemically activated C(1) site. Based on these considerations, we suggest that the energy randomization in the ethylpropargylene intermediate is likely to be incomplete; this finding is similar to the carbon–propargyl and carbon–1,2-butadiene systems in which an energy transfer over four bonds was suggested to be of only minor importance. Rather than undergoing an atomic hydrogen elimination,

ethylpropargylene could fragment to C_2H_5 + l-C_3H via a homolytic carbon–carbon bond rupture. This reaction is exoergic by 39.1 kJ mol^{-1}.

Although these considerations are only qualitative, they might be transferred also to smaller systems such as C–C_2H (section 4.1.1, figure 15 (*a*)), C–C_2H_2 (section 4.1.2, figure 15 (*b*)) and C–C_2H_3 (section 4.2.1, figure 15 (*f*)). In particular, the impact-parameter-dependent formation of distinct intermediates and their inherently different lifetimes of the propargylene species was discussed extensively (section 4.1.2). Likewise, future crossed-beams experiments should investigate the role of discrete CCCH and HCCCH$_2$ intermediates with the reacting carbon atom located at C(1) or C(2).

5.4. *Direct versus indirect scattering dynamics*

The investigations provided also important trends on indirect versus direct reactive scattering dynamics involved in the reactions of atomic carbon with unsaturated hydrocarbon species. The electronic structure calculations show explicitly that each decomposing intermediate is stabilized by a few hundred kilojoules per mole with respect to the separated reactants. These features should be reflected in indirect scattering dynamics via strongly bound intermediates. However, the actual crossed-beams experiments demonstrate that these considerations are not entirely correct. The C–C_2H_2 and C–C_2H_4 systems as the prototype reactions of carbon atoms with the simplest closed-shell alkyne and alkene follow not only indirect but also direct dynamics through extremely short-lived reaction intermediates which do not experience the deep potential energy well. As the collision energy increases, those microchannels involving direct stripping dynamics are quenched, and indirect dynamics become more significant (sections 4.1.2 and 4.2.2). Substituting one or two hydrogen atoms by a methyl group leads to an enhanced lifetime of the fragmenting intermediates in the C–CH_3CCH system (section 4.1.4), C–CH_3CCCH_3 system (section 4.1.5) and $H_2CCH(CH_3)$ system (section 4.2.5). The dynamics are entirely indirect and involve long-lived intermediates; as the collision energy rises, the dynamics change towards 'osculating complex patterns', that is lifetimes of the intermediates similar to their rotational periods; this trend supports a decreasing lifetime of the intermediates with rising collision energy. Quite interestingly, the transition to the even more complex systems C–C_6H_6 (section 4.3) and C–$H_2CCCH(CH_3)$ (section 4.2.7) does not correlate automatically with an increased lifetime of the reaction intermediates as the number of oscillators rises. With increasingly higher collision energy, the reaction dynamics change from indirect via long-lived intermediates to a direct type; the centre-of-mass angular distributions become increasingly more backward scattered as smaller impact parameters become more important. Altogether, these considerations make it clear that a careful comparison between experiments and theory is crucial to unravel the reaction dynamics of polyatomic systems comprehensively.

6. Conclusions

This review discussed recent experimental and theoretical studies of reactions of carbon atoms with various unsaturated hydrocarbons and their radicals. All reactions are fast close to gas kinetic limits, are initiated via an addition of the carbon atom to the π system and have no entrance barrier. The latter emphasizes the unique chemistry of atomic carbon as related reactions of ground-state oxygen and

nitrogen with closed-shell unsaturated molecules involve significant barriers [343]. With the exception of the $C–C_2H_2$ system, which also shows a significant fraction of molecular hydrogen elimination, these reactions are dominated by an carbon atom versus hydrogen atom exchange mechanism; in some systems, homolytic cleavages of carbon–carbon bonds present additional decomposition routes of typically a few per cent at the most. The polyatomic products of the crossed-beams reactions are highly hydrogen deficient and can be categorized into three groups of RSFRs which are strongly suggested suitable precursors to form the first (substituted) aromatic ring molecule, polycyclic aromatic hydrocarbon-like species and soot. These reaction products are, firstly, propargyl and its derivatives (propargyl; 1- and 3-methyl-propargyl; 1- and 3-vinylpropargyl), secondly, n-C_4H_3 and substituted species (n-C_4H_3; 1- and 3-methylbutatrienyl) and, finally, five C_5H_5 isomers (1- and 3-methylbutatrienyl; 1,3-butadienyl-2; 1- and 3-methylbutatrienyl (figure 16)). Here, radical–radical reactions of substituted propargyl might synthesize methylbenzene (toluene), o- and p-dimethylbenzene (xylene), o- and p-methylvinylbenzene, and o- and p-divinylbenzene [344] whereas collisions of acetylene with species of the substituted C_4H_3 radicals lead to benzene and toluene. In particular, distinct C_4H_6 isomers form particular C_5H_5 isomers which have not been incorporated into kinetic reaction networks modelling the formation of PAHs and carbonaceous nanoparti-cles in combustion flames and extraterrestrial environments. More than once, combustion chemists, those using chemical vapour deposition processes, and astrophysicists have employed similar reaction networks to explain the chemistry of these environments; multicomponent models of carbon cluster growth, the correlation with PAH and soot formation, and the stepwise build-up of nanoscale diamonds are examples [345–350]. We identified further miscellaneous reaction intermediates. Although these rovibrationally excited structures (except for the
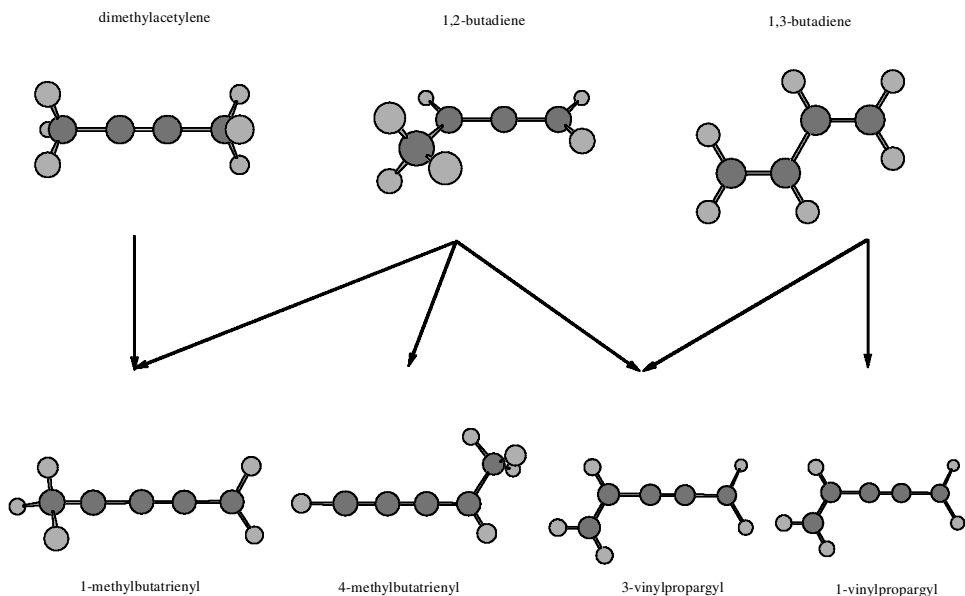

Figure 16. Reaction products from binary collisions of atomic carbon with three C_4H_6 isomers.

cyclic C_7D_6 adduct) fragment solely before a third-body collision takes place in low-density crossed-beams experiments and, in molecular clouds, the conditions are more diverse in combustion processes. Here, number densities of typically 10^{17} cm^{-3} prevail at temperatures of a few thousand kelvins, and third-body reactions can stabilize the involved intermediates efficiently. In the interstellar medium, temperatures can be as low as 10 K (cold molecular clouds) but can increase also up to 4000 K in shocked regions as well as in outflows of carbon stars close to the photosphere [351].

Giving the great importance of these hydrogen-deficient RSFRs, future experimental investigations of this reaction class should be extended to the identification of lower-mass fragments such as methyl, vinyl, ethylene, acetylene and carbene, to name just a few. These channels have important implications to the overall carbon budget of the (extra)terrestrial environments to be modelled. Although low-mass fragments in crossed-beams reactions involving atomic oxygen and unsaturated hydrocarbons can be detected easily employing the 'universal mass spectrometric detector' [352, 353], their identification in the corresponding C_xH_y systems is prevented. Here, substantial background counts from dissociative ionization of reactant molecules in the electron impact ionizer themselves makes it impracticable to detect low-mass products if they have the same mass-to-charge ratio as the reagent fragments. Therefore, significant experimental improvements are crucial. As resonant or non-resonant ionization of these small fragments is often known, they might be detected via imaging techniques [354] or, employing tunable ultraviolet–vacuum ultraviolet synchrotron radiation, via a quadrupole mass spectrometer in the TOF mode. This is in strong contrast with the heavy reaction products formed via the carbon–hydrogen exchange mechanism, whose spectroscopic properties and hence laser-based detection schemes are mostly elusive. Therefore, a hybride machine coupling a conventional mass spectrometry detection of the heavy products ('universal detector') with a spectroscopic assignment of the low-mass fragments employing imaging techniques is clearly desirable. The results from this truly universal crossed-beams machine will ultimately help to control PAH and nano-particle formation, will assist to develop innovative technologies in nanofabrication, chemical vapour deposition, semiconductor manufacturing and combustion processes and will revolutionize the understanding of crucial industrial and astro-chemical processes.

References

[1] CIAJOLO, A. *et al.*, 2001, *Combust. Flame*, **125**, 1225.
[2] HWANG, J. Y., and CHUNG, S. H., 2001, *Combust. Flame*, **125**, 752.
[3] FIALKOV, A. B., DENNEBAUM, J., and HOMANN, K. H., 2001, *Combust. Flame*, **125**, 763.
[4] WEILMÜNSTER, P., LKELLER, A., and HOMANN, K. H., 1998, *Combust. Flame*, **116**, 62.
[5] RICHTER, H. *et al.*, 2001, *J. phys. Chem.* A, **105**, 1561.
[6] SIEGMANN, K., and SATTLER, J., 2000, *Chem. Phys.*, **112**, 698.
[7] BÖHM, H., and JANDER, H., 1991, *Phys. Chem. chem. Phys.*, **1**, 3775.
[8] D'ANNA, A., VIOLI, A., D'ALESSIO, A., and SAROFIM, F., 2001, *Combust. Flame*, **127**, 1995.
[9] GREEN, S., 1981, *A. Rev. phys. Chem.*, **32**, 103.
[10] BAUKAL, C. E., 1998, *Oxygen-enhanced Combustion* (Boca Raton, Florida: CRC Press).
[11] BAIRD, C., 1999, *Environmental Chemistry* (New York: W. H. Freeman).
[12] FINLAYSON-PUITTS, B. J., and PITTS, J. N., 1997, *Science*, **276**, 1045.
[13] OLEINIK, I. I., PETTIFOR, D. G., SUTTON, A. P., BUTLER, J. E., and DIAM. R. E., 2000, *Materials*, **9**, 241.
[14] LöWE, A. G., HARTLIEB, A. T., BRAND, J., ATAKAN, B., and KOHSE-HöINGHAUS, K., 1999*, Combust. Flame*, **118**, 37.
[15] FRENKLACH, M., and SKOKOV, S., 1997, *J. Phys. Chem.* B, **101**, 3025.
[16] FOORD, J. S., LOH, K. P., SINGH, N. K., JACKMAN, R. B., and DAVIES, G. J., 1996, *J. Cryst. Growth*, **164**, 208.
[17] GIRAUD, A., *et al.*, 2001, *J. Am. chem. Soc.*, **123**, 2271.
[18] BURIAK, J. M., 2001, *Angew. Chem., Int. Edn*, **40**, 532.
[19] ASHFOLD, M. N. R., *et al.*, 2001, *Phys. Chem. chem. Phys*, **3**, 3471.
[20] SMITH, J. A., CAMERON, E., ASHFOLD, M. N. R., MANKELEVICH, Y. A., and SUETIN, N. V., 2001, *Diamond Relat. Mater.*, **10,** 358.
[21] PASCOLI, G., and POLLEUX, A., 2000, *Astr. Astrophys.*, **359**, 799.
[22] HILL, H. G. M., JONES, A. P., and D'HENDECOURT, L. B., 1998, *Astr. Astrophys. Lett.*, **336**, L41.
[23] HERLIN, N., *et al.*, 1998, *Astr. Astrophys.*, **330**, 1127.
[24] FEDERMAN, S. R., and LAMBERT, D. L., 1988, *Astrophys. J.*, **328**, 777.
[25] KROTO, H. W., and MCKAY, K., 1988, *Nature*, **331**, 328.
[26] RICHTER, H., GRIECO, W., and HOWARD, J. B., 1999, *Combust. Flame*, **119**, 1.
[27] GOROFF, N. S., 1996, *Accts Chem. Res.*, **29**, 77.
[28] HOMANN, K. H., 1998, *Angew. Chem., Int. Edn*, **37**, 2434.
[29] ALLAMANDOLA, L., TIELENS, J., and BARKER, J. R., 1989, *Astrophys. J., Suppl. Ser.*, **71**, 733.
[30] DE MUIZON, M. J., D'HENDECOURT, L. B., and GEBALLE, T. R., 1990, *Astr. Astrophys.*, **235**, 367.
[31] BERNARD, J. P., D'HENDECOURT, L. B., and LEGER, A., 1998, *Astr. Astrophys.*, **220**, 245.
[32] COSSART-MAGOS, C., and LEACH, S., 1990, *Astr. Astrophys.*, **233**, 559.
[33] VERSTRAETE, L., and LEGER, A., 1992, *Astr. Astrophys.*, **2656**, 513.
[34] HUDGINS, D. M., and SANDFORD, S. A.*, 1998, J. phys. Chem.* A., **102***, 344.
[35] SALAMA, F., JOBLIN, C., and ALLAMANDOLA, L., 1995, *J. planet. Space Sci.*, **43**, 1165.
[36] MOUTOU, C., *et al.*, 2000**, *Astr. Astrophys.*, **354**, L17.
[37] JOBLIN, C., *et al.*, 1995, *Astr. Astrophys.*, **299**, 835.
[38] COUPANEC, P. L., ROUAN, D., MOUTOU, C., and LEGER, A., 1999, *Astr. Astrophys.*, **347**, 669.
[39] SCHLEMMER, S., COOK, D. J., HARRISON, J. A., WURFEL, B., CHAPMAN, W., and SAYKALLY, R. J., 1994, *Science*, **265**, 1686.
[40] JOUDAIN DE MUIZON, M., D'HENDECOURT, L. B., and GEBAKKE, T. R., 1990, *Astr. Astrophys.*, **227**, 526.
[41] EHRENREUND, P., CAMI, J., DARTOIS, E., and FOING, B. H., 1997, *Astr. Astrophys.*, **317**, L28.
[42] JOBLIN, C., TIELENS, A. G. G. M., ALLAMANDOLA, L. J., LEGER, A., D'HENDECOURT, L., GEBALLE, T. R., and BOISSEL, P., 1995, *Planet. Space Sci.*, **43**, 1189.
[43] SALAMA, F., and ALLAMANDOLA, L. J., 1993*, J. chem. Soc., Faraday Trans.*, **89**, 2277.
[44] COOK, D. J., *et al.*, 1996, *Nature*, **380,** 227.

[45] MENNELLA, V., COLANGELI, L., and BUSSOLETTI, E., 1992, *Astrophys. J.*, **391**, 45.
[46] DULEY, W. W., 1994, *Astrophys. J.*, **429**, L91.
[47] PINO, T., *et al.*, 2001, *Chem. Phys. Lett.*, **339**, 64.
[48] HALASINKI, T. M., HUDGINS, D. M., SALAMA, F., ALLAMANDOLA, L. J., and BALLY, T., 2000, *J. phys. Chem. A.*, **104**, 7484.
[49] CHILLIER, X. D. F., STONE, B. M., SALAMA, F., and ALLAMANDOLA, L. J., 1999, *J. chem. Phys.*, **111**, 449.
[50] SALAMA, F., and ALLAMANDOLA, L. J., 1992, *Nature*, **358**, 42.
[51] OOMENS, J., VAN ROIJ, A. J. A., MAIJER, G., and VON HELDEN, G., 2000, *Astrophys. J.*, **542**, 404.
[52] HUDGINS, D. M., SANDFORD, S. A., 1998, *J. Phys. Chem. A*, **102**, 329.
[53] EHRENFREUND, R P., FOING, B. H., d'HENDECOURT, L., JENNISKENS, P., and DESERT, F. X., 1995, *Astr. Astrophys.*, **299**, 213.
[54] HUDGINS, D. M., BAUSCHLICHER, C. W., ALLAMANDOLA, L. J., and FETZER, J. C., 2000, *J. Phys. chem. A*, **104**, 3655.
[55] JOBLIN, C., TIELENS, A. G. G. M., GEBALLE, T. R., and WOODEN, D. H., 1996, *Astrophys. J.*, **460**, L119.
[56] SLOAN, G. C., *et al.* 1999, *Astrophys. J. Lett.*, **513**, 65.
[57] HUDGINS, D. M., and ALLAMANDOLA, L. J., 1997, *J. phys. Chem. A*, **101**, 3472.
[58] BAUCHLICHER, C. W., and LANGHOFF, S. R., 1997, *Spectrochim Acta* A., **53**, 1225.
[59] HUDGINS, D. M., SANDFORD, S. A., and ALLAMANDOLA, L. J., 1994, *J. phys. Chem.*, **98**, 4243.
[60] HUDGINS, D. M., and ALLAMANDOLA, L. J., 1995, *J. phys. Chem.*, **99**, 8978.
[61] ROBINSON, M. S., BEEGLE, L. W., and WDOWIAK, T. J. 1997, *Astrophys. J.*, **474**, 474.
[62] SALAMA, F., JOBLIN, C., and ALLAMANDOLA, L. J., 1994, *J. chem. Phys.*, **101**, 10 252.
[63] HUDGINS, D. M., and SANDFORD, S. A., 1998, *J. phys. Chem. A*, **102**, 353.
[64] COOK, D. J., and SAYKALLY, R. J., 1998, *Astrophys. J.*, **493**, 793.
[65] PARISEL, O., BERTHIER, G., and ELLINGER, Y., 1992, *Astr. Astrophys.*, **266**, L1.
[66] LEE, W., and WDOWIAK, T. J., 1993, *Astrophys. J.*, **410**, L127.
[67] SALAMA, F., and ALLAMANDOLA, L. J., 1992, *Astrophys. J.*, **395**, 301.
[68] SCZEPANSKI, J., and VALA, M., 1993, *Nature*, **363**, 699.
[69] HUDGINS, D. M., and ALLAMANDOLA, L. J., 1999, *Astrophys. J. Lett.*, **516**, 41.
[70] ROMANINI, D., *et al*, 1999, *Chem. Phys. Lett.*, **303**, 165.
[71] BRECHINGNAC, P., and PINO, T., 1999, *Astr. Astrophys.*, **343**, L49.
[72] BERNSTEIN, M. P., SANDFORD, S. A., and ALLAMANDOLA, L. J., 1996, *Astrophys. J.*, **472**, L127.
[73] PAUZAT, F., TALBI, D., and ELLINGER, Y., 1997, *Astrn. Astrophys.*, **319**, 318.
[74] BAUSCHLICHER, C. W., and LANGHOFF, S. R., 1998, *Chem. Phys.*, **234**, 79.
[75] DE MUIZON, M. J., d'HENECOURT, L. B., GEBALLE, T. R., 1990, *Astr. Astrophys.*, **227**, 526.
[76] BUCH, V., 1989, *Astrophys. J.*, **343**, 208.
[77] SEAHRA, S. S., and DULEY, W. W., 1999, *Astrophys. J.*, **520**, 719.
[78] SNOW, T. P., and WITT, A. N., 1995, *Science*, **270**, 1455.
[79] JOBLIN, C., LEGER, A., and MARTIN, P., 1992, *Astrophys. J. Lett.*, **393**, 79.
[80] SALAMA, F., *et al.*, 1999, *Astrophys. J.*, **526**, 265.
[81] HONY, S., *et al.*, 2001, *Astr. Astrophys.*, **370**, 1030.
[82] NATTA, A., and KRUGEL, E., 1995, *Astr. Astrophys.*, **302**, 849.
[83] ROELFSEMA, P. R., *et al.*, 1996, *Astr. Astrophys.*, **315**, L289.
[84] HANNER, M. S., TOKUNAGA, A. T., and GEBALLE, T. R., 1992, *Astrophys. J. Lett.*, **395**, 111.
[85] SCHUTTE, W. A., TIELENS, A. G. G. M., ALLAMANDOLA, L. J., COHEN, M., and WOODEN, D. H., 1990, *Astrophys. J.*, **360**, 577.
[86] MOLSTER, F. J., *et al.*, 1996, *Astr. Astrophys.*, **315**, L373.
[87] SIEBENMORGEN, R., and KRUGEL, E., 1992, *Astr. Astrophys.*, **259**, 614.
[88] COHEN, M., *et al.*, 1999, *Astrophys. J. Lett.*, **513**, 135.
[89] ALLAIN, T., SEDLMAYR, E., and LEACH, S., 1997, *Astr. Astrophys.*, **323**, 163.
[90] MOLSTER, F. J., 1996, *Astr. Astrophys. L.*, **315**, 373.
[91] TIELENS, A. G. G. M., 1997, *Astrophys. Space Sci.*, **251**, 1.

[92] BEINTEMA, D., 1996, *Astr. Astrophys.* A, **315**, L369.
[93] BEINTEMA, D. A., VAN DEN ANCKER, M. E., and WATERS, L. B. F. M., *et al.*, 1996, *Astr. Astrophys.*, **315**, L369.
[94] BUSS, R. H., TIELENS, A. G. G. M., and SNOW, T. P., 1991, *Astrophys. J.*, **372**, 281.
[95] DULEY, W. W., and SEAHRA, S., 1998, *Astrophys. J.*, **507**, 874.
[96] SCOTT, A., and DULEY, W. W., 1996, *Astrophys. J. Lett.*, **472**, 123.
[97] MENNELLA, V., *et al.*, 2001, *Astr. Astrophys.*, **367**, 335.
[98] DULEY, W. W., 2000, *Astrophys. J.*, **528**, 841.
[99] COLANGELI, L., MENNELLA, V., BARATTA, G. A., BUSSOLETTI, E., and STRAZULLA, G., 1992, *Astrophys. J.*, **396**, 369.
[100] SONNENTRUCKER, P., CAMI, J., EHRENFREUND, P., and FOING, B. H., 1997, *Astr. Astrophys.*, **327,** 1215.
[101] SCOTT, A. D., DULEY, W. W., and JAHANI, H. R., 1997, *Astrophys. J. Lett.*, **490**, 175.
[102] SCHNAITER, M., *et al.*, 1999, *Astrophys. J.*, **519**, 687.
[103] DULEY, W. W., SCOTT, A. D., SEAHRA, S., and DADSWELL, G., 1998, *Astrophys. J.*, **503**, L183.
[104] GALAZUTDINOV, G. A., *et al.*, 2000, *Mon. Not. R. Astr. Soc.*, **317**, 750.
[105] EHRENFRUEND, P., and FOING, B. H., 1995, *Planet. Space Sci.*, **43**, 1183.
[106] PETRIE, S., and BOHME, D. K., 2000, *Astrophys. J.*, **540**, 869.
[107] MOUTOU, C., SELLGREN, K., VERSTRAETE, L., and LEGER, L., 1999, *Astr. Astrophys.* A, **347**, 949.
[108] CLAYTON, G. S., 1995, *Astr. J.*, **109**, 2069.
[109] HERBIG, G. H., 2000, *Astrophys. J.*, **542**, 334.
[110] GUILLOIS, O., LEDOUX, G., and REYNAUD, C., 1999, *Astrophys. J. Lett.*, **521**, 133.
[111] ANDERSEN, A. C., *et al.*, 1998, *Astr. Astrophys.*, **330**, 1080.
[112] HILL, H. G. M., JONES, A. P., and D'HENDECOURT, L. B., 1998, *Astr. Astrophys.*, **336**, L41.
[113] LIN, Y. T., MISHRA, R. K., and LEE, S. L., 1999, *J. phys. Chem.* B, **103**, 3151.
[114] 2001, *Discuss. Faraday Soc.*, **119**.
[115] FOLTIN, M., *et al.*, 1997, *J. chem. Phys.*, **107**, 6246.
[116] PASCOLI, G., and POLLEUX, A., 2000, *Astr. Astrophys.*, **359**, 799.
[117] LIN, Y. T., MISHRA, R. K., and LEE, S. L., 1999, *J. phys. Chem.* B, **103**, 3151.
[118] FRENKLACH, M., and FEIGELSON, E. D., 1989, *Astr. Astrophys.*, **341**, 372.
[119] RICHTER, H., *et al.*, 2001, *J. phys. Chem.* A, **105**, 1561.
[120] WANG, R., CADMAN, P., 1998, *Combust. Flame*, **112**, 359.
[121] BAUSCHLICHER, C. W., and RICCA, A., 2000, *Chem. Phys. Lett.*, **326**, 283.
[122] FROCHTENICHT, R., HIPPLER, H., TROE, J., and TOENNIES, J. P., 1994, *J. Photobiol.* A, **80**, 33.
[123] MORTER, C. L., *et al.*, 1994, *J. phys. Chem.*, **98**, 7029.
[124] ADAMSON, J. D., *et al.*, 1996, *J. phys. Chem.*, **100**, 2125.
[125] CHERCHNEFF, I., BARKER, J. R., and TIELENS, A. G. G. M., 1992, *Astrophys. J.*, **401**, 269.
[126] CHERCHNEFF, I., and BARKER, J. R., 1992, *Astrophys. J.*, **394**, 703.
[127] BLITZ, A., *et al.*, 2000, *Phys. Chem. chem. Phys.*, **2**, 805.
[128] MARINOV, N. M., CASTALDI, M. J. D., MELIUS, C. F., and TSANG, W., 1997, *Combust. Sci. Technol.*, **128**, 295.
[129] BABUSHOK, V., and TSANG, W., 2000, *Combust. Flame*, **123**, 488.
[130] KAZAKOV, A., and FRENKLACH, M., 1998, *Combust. Flame*, **112**, 270.
[131] WEILMUNSTER, P., KELLER, A., and HOMANN, K. H., 1999, *Combust. Flame*, **116**, 62.
[132] MCENALLY, C. S., and PFEFFERLE, L. D., 1998, *Combust. Flame*, **112**, 545.
[133] OLTEN, N., and SENKAN, S., 1999, *Combust. Flame*, **118**, 500.
[134] MARINOV, N. M., *et al.*, 1996, *Combust. Sci. Technol.*, **116–117**, 211.
[135] MELTON, T. R., INAL, F., and SENKAN, S. M., 2000, *Combust. Flame*, **121**, 671.
[136] MCENALLY, C. S., and PFEFFERLE, L. D., 2000, *Combust. Flame*, **123**, 344.
[137] MARINOV, N. M., *et al.*, 1998, *Combust. Flame*, **114**, 192.
[138] ARRINGTON, C. A., RAMOS, C., ROBINSON, A. D., and ZWIER, T. S., 1998, *J. phys. Chem.* A, **102**, 3315.
[139] KEENE, J., *et al.*, 1993, *Astrophys. J.*, **415**, L131.

[140] VAN DER KEEN, W. E. C. J., HUGGINS, P. J., and MATTHEWS, H. E., 1998, *Astrophys. J.*, **505**, 749.

[141] INGALLIS, J. G., *et al.*, 1997, *Astrophys. J.*, **479**, 296.

[142] WILSON, C. D., 1997, *Astrophys. J. Lett.*, **487**, 49.

[143] YOUNG, K., 1997, *Astrophys. J.*, **488**, L157.

[144] SOFIA, U. J., *et al.*, 1997, *Astrophys. J. Lett.*, **482**, 105.

[145] WHITE, G. J., and SANDELL, G., 1995, *Astr. Astrophys.*, **299**, 179.

[146] HUNG, W. C., HUANG, M. L., LEE, Y. C., and LEE, Y. P., 1995, *J. chem. Phys.*, **103**, 9941.

[147] D'ANNA, A., VIOLI, A., and D'ALLESSIO, A., 2000, *Combust. Flame*, **121**, 418.

[148] D'ANNA, A., and VIOLI, A., 1998, *Proc. Combust. Inst.*, **27**, 425.

[149] FARAVELLI, T., GOLDANIGA, A., and RANZI, E., 1998, *Proc. Combust. Inst.*, **27**, 1489.

[150] APPEL, J., BOCKHORN, H., and FRENKLACH, M., 2000, *Combust. Flame*, **121**, 122.

[151] WANG, H., and FRENKLACH, M., 1997, *Combust. Flame*, **110**, 173.

[152] LINDSTEDT, R. P., and SKEVIS, G., 1996, *Proc. Combust. Inst.*, **26**, 703.

[153] LINDSTEDT, P., 1998, *Proc. Combust. Inst.*, **27**, 269.

[154] DAGAUT, P., and CATHONNET, M., 1998, *Combust. Flame*, **113**, 620.

[155] WESTMORELAND, P. R., DEAN, A. M., HOWARD, J. B., and LONGWELL, J. P., 1989, *J. phys. Chem.*, **93**, 8171.

[156] LAMPRECHT, A., ATAKAN, B., and KOHSE-HÖINGHAUS, K., 2000, *Combust. Flame*, **122**, 483.

[157] HARTLIEB, F., ATAKAN, B., and KOHSE-HÖINGHAUS, K., 2000, *Combust. Flame*, **121**, 610.

[158] ATAKAN, B., HARTLIEB, A. T., BRAND, J., and KOHSE-HÖINGHAUS, K., 1998, *Proc. Combust. Inst.*, **27**, 435.

[159] DOUTÉ C., DELFAU, J.-L., and VOVELLE, C., 1994, *Combust. Sci. Technol.*, **103**, 153.

[160] POPE, C. J., and MILLER, J. A., 2000, *Proc. Combust. Inst.*, **28**, 1579.

[161] CASTALDI, M. J., MARINOV, N. M., MELIUS, C. F., HWANG, J., SENKAN, S. M., PITZ, W. J., and WESTBROOK, C. K., 1996, *Proc. Combust. Inst.*, **26**, 693.

[162] MARINOV, N. M., PITZ, W. J., WESTBROOK, C. K., CASTALDI, M. J., and SENKAN, S. M., 1996, *Combust. Sci. Technol.*, **116–117**, 211.

[163] MELIUS, C. F., COLVIN, M. E., MARINOV, N. M., PITZ, W. J., and SENKAN, S. M., 1996, *Proc. Combust. Inst.*, **26**, 685.

[164] MILLER, J. A., VOLPONI, J. V., and PAUWELS, J.-F., 1996, *Combust. Flame*, **105**, 451.

[165] PAUWELS, J.-F., VOLPONI, J. V., and MILLER, J. A., 1995, *Combust. Sci. Technol.*, **110–111**, 249.

[166] MILLER, J. A., and MELIUS, C. F., 1992, *Combust. Flame*, **91**, 21.

[167] MELIUS, C. F., MILLER, J. A., and EVLETH, E. M., 1992, *Proc. Combust. Inst.*, **24**, 621.

[168] DAVIS, S. G., LAW, C. K., and WANG, H., 1998, *Proc. Combust. Inst.*, **27**, 305.

[169] STEIN, S. E., WALKER, J. A., SURYAN, M., and FAHR, A., 1990, *Proc. Combust. Inst.*, **23**, 85.

[170] MILLER, J. A., 1984, *Proc. Combust. Inst.*, **20**, 461.

[171] RICHTER, H., and HOWARD, J. B., 2000, *Prog. Energy Combust. Sci.*, **26**, 565.

[172] ATKINSON, D. B., and HUDGENS, J. W., 1999, *J. phys. Chem. A*, **103**, 4242.

[173] HAHN, D. K., KLIPPENSTEIN, S. J., and MILLER, J. A., 2001, *Discuss. Faraday Soc.*, **119**, 79.

[174] SLAGLE, I. R., and GUTMAN, D., 1986, *Proc. Combust. Inst.*, **21**, 875.

[175] KERN, R. D., SINGH, H. J., and WU, C. H., 1988, *Int. J. chem. Kinetics*, **20**, 731.

[176] ALKEMADE, V., and HOMANN, K., 1989, *Z. phys. Chem., Neue Folge*, **161**, 19.

[177] HIDAKA, Y., NAKAMURA, T., MIYAUCHI, A., SHIRAISHI, T., and KAWANO, H., 1989, *Int. J. chem. Kinetics*, **29**, 643.

[178] MORTER, C., FARHAT, S., ADAMSON, J., GLASS, G., and CURL, R., 1994, *J. phys. Chem.*, **98**, 7029.

[179] KERN, R. D., CHEN, H., KIEFER, J. H., and MUDIPALLI, P. S., 1995, *Combust. Flame*, **100**, 177.

[180] MILLER, J. A., and KLIPPENSTEIN, S. J., 2001, *J. phys. Chem. A*, **105**, 7254.

[181] WU, C. J., and KERN, R. D., 1987, *J. phys. Chem.*, **91**, 6291.

[182] ADAMSON, J. D., MORTER, C. L., DeSAIN, J. D., GLASS, G. P., and CURL, R. F., 1996, *J. phys. Chem.*, **100**, 2125.

[183] PEETERS, J., VANHAELEMEERSCH, J., VAN HOEMISSEN, J., BORMS, R., and VERMEYLEN, D., 1989, *J. phys. Chem.*, **93**, 3892.

[184] CANOSA-MAS, C. E., ELLIS, M., FREY, H. M., and WALSH, R., 1984, *Int. J. chem. Kinetics*, **16**, 1103.

[185] THORNE, L. R., BRANCH, M. C., and CHANDLER, D. W., 1986, *Proc. Combust. Inst.*, **21**, 965.

[186] KAISER, R. I.; LEE, Y. T., and SUITS, A. G., 1996, *J. chem. Phys.*, **105**, 8705.

[187] MADDEN, L. K., MOSKALEVA, L. V., KRISTYAN, S., and LIN, M. C., 1997, *J. phys. Chem. A*, **101**, 6790.

[188] WALSH, S. P., 1995, *J. chem. Phys.*, **103**, 8544.

[189] FRENKLACH, M., CLARY, D. W., GARDINER, W. C., and STEIN, S. E., 1984, *Proc. Combust. Inst.*, **20**, 887.

[190] FRENKLACH, M., CLARY, D. W., GARDINER, W. C., and STEIN, S. E., 1986, *Proc. Combust. Inst.*, **21**, 1067.

[191] WANG, H., and FRENKLACH, M., 1994, *J. phys. Chem.*, **98**, 11 465.

[192] BITTNER, J. D., HOWARD, J. B., 1981, *Proc. Combust. Inst.*, **18**, 1105.

[193] DEAN, A. M., 1990, *J. phys. Chem.*, **94**, 1432.

[194] MARINOV, N. M., PITZ, W. J., WESTBROOK, C. K., VINCITORE, A. M., CASTALDI, M. J., SENKAN, S. M., and MELIUS, C. F., 1998, *Combust. Flame*, **114**, 192.

[195] MOSKALEVA, L. V., MEBEL, A. M., and LIN, M. C., 1996, *Proc. Combust. Inst.*, **26**, 521.

[196] MADDEN, L. K., MEBEL, A. M., LIN, M. C., and MELIUS, C. F., 1996, *J. Phys. org. Chem.*, **9**, 801.

[197] GAYNOR, B. J., GILBERT, R. G., KING, K. D., and HARMAN, P. J., 1981, *Aust. J. Chem.*, **34**, 449.

[198] LIN, C.-Y., and LIN, M. C., 1985, *Int. J. chem. Kinetics*, **17**, 1025; 1986, *J. phys. Chem.*, **90**, 425.

[199] HAIDER, N., and HUSAIN, D., 1993, *J. chem. Soc., Faraday Trans.*, **89**, 7.

[200] HAIDER, N., and HUSAIN, D., 1993, *Int. J. Chem. Kinetics*, **25**, 423.

[201] HAIDER, N., and HUSAIN, D. Z., 1992, *Phys. Chem.*, **176**, 133.

[202] HUSAIN, D., and IOANNOU, A. X., 1997, *J. chem. Soc., Faraday Trans.*, **93**, 3625.

[203] HAIDER, N., and HUSAIN, D., 1993, *J. Photobiol. A, Chem.*, **70**, 119.

[204] HUSAIN, D., and KIRSCH, L. J., 1971, *J. chem. Soc., Faraday Trans.*, **67**, 2025.

[205] HUSAIN, D., and YOUNG, A. N., 1975, *J. chem. Soc., Faraday Trans.*, **71**, 525.

[206] HAIDER, N., and HUSAIN, D., 1993, *Ber. Bunsenges. phys. Chem.*, **97**, 571.

[207] HUSAIN, D., 1993, *J. chem. Soc., Faraday Trans.*, **89**, 2164.

[208] BERGEAT, A., CALVO, T., DORTHE, G., and LOISON, J. C., 1999, *Chem. Phys. Lett.*, **308**, 7.

[209] BERGEAT, A., and LOISON, J. C. 2001, *Phys. Chem. chem. Phys.*, **3**, 2038.

[210] CLARY, D. C., HAIDER, N., HUSAIN, D., and KABIR, M., 1994, *Astrophys. J.*, **422**, 416.

[211] CHASTAING, D., JAMES, P. L., SIMS, I. R., and SMITH, I. W. M., 1999, *Phys. Chem. chem. Phys.*, **1**, 2247.

[212] CHASTAING, D., LE PICARD, S. D., SIMS, I. R., and SMITH, I. W. M., 2001, *Astr. Astrophys.*, **365**, 241.

[213] ROWE, B., and PARENT, D. C., 1995, *Planet. Space Sci.*, **43**, 105.

[214] SIMS, I. R., *et al.*, 1993, *Chem. Phys. Lett.*, **211**, 461.

[215] ROWE, B., CANOSA, A., and SIMS, I. R., 1993, *J. chem. Soc., Faraday Trans.*, **89**, 2193.

[216] SMITH, I. W. M., SIMS, I. R., and ROWE, B. R., 1997, *Chem. Eur. J.*, **3**, 1925.

[217] CHASTAING, D., JAMES, P. L., SIMS, I. R., and SMITH, I. W. M., 1996, *Discuss. Faraday Soc.*, **109**, 165.

[218] SIMS, I. R., and SMITH, I. W. M., 1995, *A. Rev. phys. Chem.*, **46**, 109.

[219] SMITH, I. W. M., 1995, *Int. J. Mass Spectrosc. Ion Processes*, **149–150**, 231.

[220] SMITH, I. W. M., and ROWE, B. R., 2000, *Accts Chem. Res.*, **33**, 261.

[221] LEE, Y. T., 1988, *Atomic and Molecular Beams*, Vol. 1, edited by G. Scoles (Oxford University Press), p. 553.

[222] SCOLES, G. (editor), 1992, *Atomic and Molecular Beams*, Vol. 2 (Oxford University Press).
[223] LEVINE, R. D., and BERNSTEIN, R. B., 1987, *Molecular Reactions and Chemical Reactivity* (Oxford University Press).
[224] KAISER, R. I., and BALUCANI, N., 2001, *Accts Chem. Res.*, **34**, 699.
[225] KAISER, R. I., 2002, *Chem. Rev.*
[226] KAISER, R. I., and SUITS, A. G., 1995, *Rev. scient. Instrum.*, **66**, 5405.
[227] CASAVECCHIA, P., *et al.*, 2001, *Discuss. Faraday Soc.*, **119**, 27.
[228] NAULIN, C., and COSTES, M., 1999, *Chem. Phys. Lett.*, **310**, 231.
[229] NAULIN, C., and COSTES, M. J., 1995, *Chin. Chem. Soc.*, **42**, 215.
[230] WERNER, H.-J., and KNOWLES, P. J., 1988, *J. chem. Phys.*, **89**, 5803.
[231] KNOWLES, P. J., and WERNER, H.-J., 1988, *Chem. Phys. Lett.*, **145**, 514.
[232] PURVIS, G. D., and BARTLETT, R. J., 1982, *J. chem. Phys.*, **76**, 1910.
[233] POPLE, J. A., HEAD-GORDON, M., and RAGHAVACHARI, K., 1987, *J. chem. Phys.*, **87**, 5968.
[234] DUNNING, T. H., JR., 1989, *J. chem. Phys.*, **90**, 1007.
[235] KRISHNAN, R., and POPLE, J. A., 1978, *Int. J. quantum Chem.*, **14**, 91.
[236] CURTISS, L. A., RAGHAVACHARI, K., TRUCKS, G. W., and POPLE, J. A., 1991, *J. chem. Phys.*, **94**, 7221.
[237] CURTISS, L. A., RAGHAVACHARI, K., and POPLE, J. A., 1993, *J. chem. Phys.*, **98**, 1293.
[238] POPLE, J. A., HEAD-GORDON, M., FOX, D. J., RAGHAVACHARI, K., and CURTISS, L. A., 1989, *J. chem. Phys.*, **90**, 5622.
[239] CURTISS, L. A., JONES, C., TRUCKS, G. W., RAGHAVACHARI, K., and POPLE, J. A., 1990, *J. chem. Phys.*, **93**, 2537.
[240] CURTISS, L. A., REDFERN, P. C., RAGHAVACHARI, K., RASSOLOV, V., and POPLE, J. A., 1999, *J. chem. Phys.*, **110**, 4703.
[241] BABOUL, A. G., CURTISS, L. A., REDFERN, P. C., and RAGHAVACHARI, K., 1999, *J. chem. Phys.*, **110**, 7650.
[242] CURTISS, L. A., RAGHAVACHARI, K., REDFERN, P. C., BABOUL, A. G., and POPLE, J. A., 1999, *Chem. Phys. Lett.*, **314**, 101.
[243] CURTISS, L. A., RAGHAVACHARI, K., REDFERN, P. C., and POPLE, J. A., 2000, *J. chem. Phys.*, **112**, 1125.
[244] CURTISS, L. A., RAGHAVACHARI, K., REDFERN, P. C., and POPLE, J. A., 2000, *J. chem. Phys.*, **112**, 7374.
[245] REDFERN, P. C., ZAPOL, P., CURTISS, L. A., and RAGHAVACHARI, K., 2000, *J. phys. Chem.* A, **104**, 5850.
[246] CURTISS, L. A., REDFERN, P. C., RAGHAVACHARI, K., and POPLE, J. A., 2001, *J. chem. Phys.*, **114**, 108.
[247] CURTISS, L. A., RAGHAVACHARI, K., REDFERN, P. C., KEDZIORA, G., and POPLE, J. A., 2001, *J. phys. Chem.* A, **105**, 227.
[248] CURTISS, L. A., REDFERN, P. C., RASSOLOV, V., KEDZIORA, G., and POPLE, J. A., 2001, *J. chem. Phys.*, **114**, 9287.
[249] CURTISS, L. A., RAGHAVACHARI, K., REDFERN, P. C., and POPLE, J. A., 1997, *J. chem. Phys.*, **106**, 1063.
[250] CURTISS, L. A., REDFERN, P. C., RAGHAVACHARI, K., and POPLE, J. A., 1998, *J. chem. Phys.*, **109**, 42.
[251] MEBEL, A. M., MOROKUMA, K., and LIN, M. C., 1995, *J. chem. Phys.*, **103**, 7414.
[252] BAUSCHLICHER, C. W., JR, and PARTRIDGE, H., 1995, *J. chem. Phys.*, **103**, 1788.
[253] MEBEL, A. M., MOROKUMA, K., LIN, M. C., and MELIUS, C. F., 1995, *J. phys. Chem.*, **99**, 1900.
[254] BECKE, A. D., 1993, *J. chem. Phys.*, **98**, 5648.
[255] LEE, C., YANG, W., and PARR, R. G., 1988, *Phys. Rev.* B, **37**, 785.
[256] SCOTT, A. P., and RADOM, L., 1996, *J. phys. Chem.*, **100**, 16 502.
[257] GONZALES, C., and SCHLEGEL, H. B., 1989, *J. chem. Phys.*, **90**, 2154.
[258] DUNN, K., and MOROKUMA, K., 1995, *J. chem. Phys.*, **102**, 4904.
[259] CUI, Q., 1998, PhD Thesis, Emory University, Atlanta, Georgia.
[260] EYRING, H., LIN, S. H., and LIN, S. M., 1980, *Basic Chemical Kinetics* (New York: Wiley).

[261] BAER, T., and HASE, W. L., 1996, *Unimolecular Reaction Dynamics: Theory and Experiment* (Oxford: University Press).
[262] STEINFELD, J. I., FRANCISCO, J. S., and HASE, W. L., 1999, *Chemical Kinetics and Dynamics* (Englewood Cliffs, New Jersey: Prentice-Hall).
[263] ROBINSON, P. J., and HOLBROOK, K. A., 1972, *Unimolecular Reactions* (New York: Wiley).
[264] BALUCANI, N., LEE, H. Y., MEBEL, A., LEE, Y. T., and KAISER, R. I., 2001, *J. chem. Phys.*, **115**, 5107.
[265] KAISER, R. I., MEBEL, A. M., LEE, Y. T., and CHANG, A. H. H., 2001, *J. chem. Phys.*, **115**, 5117.
[266] KAISER, R. I., ASVANY, O., LEE, Y. T., BETTINGER, H. F., SCHLEYER, P. V. R., and SCHAEFER III, H. F., 2000, *J. chem. Phys.*, **112**, 4994.
[267] KAISER, R. I., MEBEL, A. M., and LEE, Y. T., 2001, *J. chem. Phys.*, **114**, 231.
[268] KAISER, R. I., NGUYEN, T. L., MEBEL, A. M., and LEE, Y. T., 2002, *J. chem. Phys.*, **116**, 1318.
[269] MAYNE, H. R., 1991, *Int. Rev. phys. Chem.*, **10**, 107.
[270] SCHATZ, G. C., 1995, *J. phys. Chem.*, **99**, 516.
[271] CASAVECCHIA, P., 2000, *Rep. Prog. Phys.*, **63**, 355.
[272] AOIZ F. J., BANARES, L., HERRERO, V. J., and RABANOS, V. S., 1994, *J. chem. Phys.*, **98**, 10 665.
[273] AOIZ, F.J., *et al.*, 1995, *J. chem. Phys.*, **102**, 9248.
[274] AOIZ, F. J., *et al.*, 1996, *Chem. Phys. Lett.*, **254**, 341.
[275] ALAGIA, M., *et al.*, 2000, *Phys. Chem. chem. Phys.*, **2**, 599.
[276] BALUCANI, N., *et al.*, 2000, *Chem. Phys. Lett.*, **328**, 500.
[277] AOIZ, F. J., *et al.*, 2001, *J. chem. Phys.*, **115**, 2074.
[278] KEOGH, W. J., *et al.*, 1992, *Chem. Phys. Lett*, **195**, 144.
[279] BLAIS N. C., *et al.*, 1989, *J. chem. Phys.*, **91**, 1038.
[280] PEDERSON, L. A., *et al.*, 1999, *J. chem. Phys*, **110**, 9091.
[281] BALUCANI, N., *et al.*, 2001, *J. phys. Chem.* A, **105**, 2414.
[282] ALAGIA, M., *et al.*, 1998, *J. chem. Phys.*, **108**, 6698.
[283] ALEXANDER, A. J., AOIZ, F. J., BROUARD, M., and SIMONS, J. P., 1996, *Chem. Phys. Lett.*, **256**, 561.
[284] HSU, Y. T., LIU, K., PEDESRSON, L. A., and SCHATZ, G. C. 1999, *J. chem. Phys.*, **111**, 7931.
[285] ZYUBIN, A. S., MEBEL, A. M., CHAO, S. D., and SKODJE, R. T., 2001, *J. chem. Phys.*, **114**, 320.
[286] CHAO, S. D., and SKODJE, R. T., 2001, *J. phys. Chem.* A, **105**, 2474.
[287] BRADLEY, K. S., SCHATZ, G. C., 1997, *J. chem. Phys.*, **106**, 8464.
[288] KUDLA, K., KOURES, A. G., HARDING, L. B., and SCHATZ, G. C., 1992, *J. chem. Phys.*, **96**, 7465.
[289] KUDLA, K., SCHATZ, G. C., and WAGNER, A. F., 1991, *J. chem. Phys.*, **95**, 1635.
[290] WU, G., *et al.*, 2000, *J. chem. Phys.*, **113**, 3150.
[291] PALMA, J., ECHAVE, J., CLARY, and D. C., 1997, *J. chem. Soc., Faraday Trans.*, **93**, 841.
[292] POGREBNYA, S. K., PALMA, J., CLARY, D. C., and ECHAVE, J., 2000, *Phys. Chem. chem. Phys.*, **2**, 693.
[293] BRADLEY, K. S., and SCHATZ, G. C., 1998, *J. chem. Phys.*, **108**, 7994.
[294] BRADLEY, K. S., and SCHATZ, G. C., 1994, *J. phys. Chem.*, **98**, 3788.
[295] KUDLA, K., and SCHATZ, G. C., 1992, *Chem. Phys. Lett.*, **193**, 507.
[296] TROYA, D., GONZALEZ, M., and SCHATZ, G. C., 2001, *J. chem. Phys.*, **114**, 8397.
[297] TROYA, D., LAKIN, M. J., SCHATZ, G. C., and GONZALEZ, M., 2001, *J. chem. Phys.*, **115**, 1828.
[298] TROYA, D., LENDVAY, G., GONZALEZ, M., and SCHATZ, G. C., 2001, *Chem. Phys. Lett.*, **343**, 420.
[299] LAKIN, M. J., *et al.*, 2001, *J. chem. Phys.*, **115**, 5160.
[300] TERHORST, M. A., SCHATZ, G. C., and HARDING, L. B., 1996, *J. chem. Phys.*, **105**, 558.
[301] SAYOS, R., OLIVA, C., and GONZALEZ, M., 2000, *J. chem. Phys.*, **113**, 6736.

[302] SAYOS, R., HERNANDO, J., PUYUELO, M. P., ENRIQUEZ, P. A., and GONZALEZ, M., 2002, *Phys. Chem. chem. Phys.*, **4**, 288.
[303] GONZALEZ, M., HERNANDO, J., MILLAN, J., and SAYOS, R., 1999, *J. chem. Phys.*, **110**, 7326.
[304] GONZALEZ, M., HERNANDO, J., BANOS, I., and SAYOS, R., 1999, *J. chem. Phys*, **111**, 8913.
[305] GONZALEZ, M., HERNANDO, J., PUYUELO, M. P., and SAYOS, R., 2000, *J. chem. Phys.*, **113**, 6748.
[306] GONZALEZ, M., *et al.*, 2001, *J. phys. Chem. A*, **105**, 9834.
[307] CLARY, D. C., 1999, *Phys. Chem. chem. Phys.*, **1**, 1173.
[308] GUADAGNINI, R., and SCHATZ, G. C., 1996, *J. phys. Chem.*, **100**, 18 944.
[309] BUONOMO, E., and CLARY, D. C., 2001, *J. phys. Chem.*, **105**, 2694.
[310] MEBEL, A. M., and KAISER, R. I., 2002, *Chem. Phys. Lett.*
[311] *NIST Chemistry WebBook* (Gauthersburg, Maryland: National Institute of Standards and Technology) http://webbook.nist.gov/.
[312] KAISER, R. I., OCHSENFELD, C., HEAD-GORDON, M., LEE, Y. T., and SUITS, A. G., 1996, *Science*, **274**, 1508.
[313] KAISER, R. I., OCHSENFELD, C., HEAD-GORDON, M., LEE, Y. T., and SUITS, A. G., 1997, *J. chem. Phys.*, **106**, 1729.
[314] OCHSENFELD, C., KAISER, R. I., SUITS, A. G., LEE, Y. T., and HEAD-GORDON, M., 1997, *J. chem. Phys.*, **106**, 4141.
[315] KAISER, R. I., LEE, Y. T., and SUITS, A. G., 1995, *J. chem. Phys.*, **103**, 10 395.
[316] BUONOMO, E., and CLARY, D. C., 2001, *J. phys. Chem. A*, **105**, 2694.
[317] KAISER, R. I., *et al.*, 2001, *Discuss. Faraday Soc.*, **199**, 51.
[318] MEBEL, A. M., JACKSON W. M., CHANG, A. H. H., and LIN S. H., 1998, *J. Am. chem. Soc.*, **120**, 5751.
[319] SCHOLEFIELD, M. R., *et al.*, 1998, *Chem. Phys. Lett.*, **288**, 487.
[320] LE, T. N., MEBEL, A. M., and KAISER, R. I., 2001, *J. comput. Chem.*, **22**, 1522.
[321] KAISER, R. I., SUN, W., SUITS, A. G., and LEE, Y. T., 1997, *J. chem. Phys.*, **107**, 8713.
[322] KIASER, R. I., STRANGES, D., LEE, Y. T., and SUITS, A. G., 1996, *J. chem. Phys.*, **105**, 8721.
[323] MEBEL, A. M., KAISER, R. I., and LEE, Y. T., 2000, *J. Am. chem. Soc.*, **122**, 1776.
[324] KAISER, R. I., STRANGES, D., LEE, Y. T., and SUITS, A. G., 1997, *Astrophys. J.*, **477**, 982.
[325] HUANG, L. C. L., LEE, H. Y., MEBEL, A. M., LIN, S. H., LEE, Y. T., and KAISER, R. I., 2000, *J. chem. Phys.*, **113**, 9637.
[326] MEBEL, A. M., KAISER, R. I., and LEE, Y. T., 2001, *J. Am. chem. Soc.*, **122**, 1776.
[327] KAISER, R. I., OCHSENFELD, C., STRANGES, D., HEAD-GORDON, M., and LEE, Y. T., 1998, *Discuss. Faraday Soc.*, **109**, 183.
[328] NGUYEN, T. L., MEBEL, A. M., and KAISER, R. I., 2001, *J. phys. Chem. A*, **105**, 3284.
[329] NGUYEN, T. L., MEBEL, A. M., LIN, S. H., and KAISER, R. I., 2002, *J. phys. Chem. A*, **105**, 11 549.
[330] LE, T. N., LEE, H. Y., MEBEL, A. M., and KAISER, R. I., 2001, *J. phys. Chem. A.*, **105**, 1847.
[331] KAISER, R. I., MEBEL, A., CHANG, A. H. H., LIN, S. H., and LEE, Y. T., 1999, *J. chem. Phys.*, **110**, 10 330.
[332] NGUYEN, T. L., MEBEL, A. M., and KAISER, 2001 (submitted).
[333] KAISER, R. I., STRANGES, D., BEVSEK, H. M., LEE, Y. T., and SUITS, A. G., 1997, *J. chem. Phys.*, **106**, 4945.
[334] NGUYEN, T. L., MEBEL, A. M., and KAISER, R. I., 2001, *J. phys. Chem. A* (submitted).
[335] MEBEL, A. M. 2002 (to be published).
[336] HAHNDORF, I., LEE, H. Y., MEBEL, A., LIN, S. H., LEE, Y. T., and KAISER, R. I., 2000, *J. chem. Phys.*, **113**, 9622.
[337] MEBEL, A. M., LIN, M. C., CHAKRABORTY, D., PARK, J., LIN, S. H., and LEE, Y. T., 2001, *J. chem. Phys.*, **114**, 8421.
[338] KAISER, R. I., LEE, H. Y., MEBEL, A. M., and LEE, Y. T., 2001, *Astrophys. J.*, **548**, 852.

[339] KAISER, R. I., HAHNDORF, I., HUANG, L. C. L., LEE, Y. T., BETTINGER, H. F., SCHLEYER, P. V. R., SCHAEFER III, H. F., and SCHREINER, P. R., 1999, *J. chem. Phys.*, **110**, 6091.

[340] HAHNDORF, I., LEE, Y. T., KAISER, R. I., VEREECKEN, L., PEETERS, J., BETTINGER, H. F., and SCHLEYER, P. V. R., SCHAEFER III, H. F., 2002, *J. chem. Phys.*, **116**, 3248.

[341] BETTINGER, H. F., SCHLEYER, P. V. R., SCHREINER, P. R., SCHAEFER III, H. F., KIASER, R. I., and LEE,, Y. T., 2000, *J. chem. Phys.*, **113**, 4250.

[342] KAISER, R. I., (unpublished).

[343] *NIST Database*, Vol. 17, *Chemical Kinetics* (Gauthersburg, Maryland: National Institute of Standards and Technology).

[344] KAISER, R. I., NGUYEN, T. L., LE, T. N., and MEBEL, A. M., 2001, *Astrophys. J.*, **561**, 858.

[345] PASCOLI, G., and POLLEUX, A., 2000, *Astr. Astrophys.*, **359**, 799.

[346] DE THIEJE, F. K., SCHERMER, J. J., and VAN ENCKEVORT, W. J. P., 2000, *Diamond Relat. Res.*, **9**, 1439.

[347] BAUKAL, C. E., 1998, *Oxygen-enhanced Combustion* (Boca Raton: Florida: CRC Press).

[348] HAUSMANN, M., and HOMANN, K. H., 1990, *Ber. Bunsenges. phys. Chem.*, **94**, 1308.

[349] HARRIS, S. J., SHIN, S. H., and GOODWIN, D. G., 1995, *Appl. Phys. Lett.*, **66**, 891.

[350] CELII, F. G., and BUTLER, J. E., 1991, *A. Rev. phys. Chem.*, **42**, 643.

[351] KAISER, R. I. 2002, *Chem. Rev.* (to be published).

[352] SHU, J. N., LIN, J. J., LEE, Y. T., and YANG, X. M., 2001, *J. chem. Phys.*, **114**, 4.

[353] SHU, J., LIN, J. J., LEE, Y. T., and YANG, X. M., 2001, *J. chem. Phys.*, **115**, 849.

[354] AHMED, M., PETERKA, D. S., and SUITS, A. G., 2000, *Chem. Phys. Lett.*, **317**, 264.